

Comparative Direct Analysis of Type Ia Supernova Spectra. IV. Postmaximum

David Branch¹, David J. Jeffery^{1,2}, Jerod Parrent^{1,3}, E. Baron¹, M. A. Troxel¹,
V. Stanishev⁴, Melissa Keithley¹, Joshua Harrison¹, and Christopher Bruner^{1,5}

ABSTRACT

A comparative study of optical spectra of Type Ia supernovae (SNe Ia) obtained near 1 week, 3 weeks, and 3 months after maximum light is presented. Most members of the four groups that were defined on the basis of maximum light spectra in Paper II (core normal, broad line, cool, and shallow silicon) develop highly homogeneous postmaximum spectra, although there are interesting exceptions. Comparisons with SYNOW synthetic spectra show that most of the spectral features can be accounted for in a plausible way. The fits show that 3 months after maximum light, when SN Ia spectra are often said to be in the nebular phase and to consist of forbidden emission lines, the spectra actually remain dominated by resonance scattering features of permitted lines, primarily those of Fe II. Even in SN 1991bg, which is said to have made a very early transition to the nebular phase, there is no need to appeal to forbidden lines at 3 weeks postmaximum, and at 3 months postmaximum the only clear identification of a forbidden line is [Ca II] $\lambda\lambda$ 7291, 7324. Recent studies of SN Ia rates indicate that most of the SNe Ia that have ever occurred have been “prompt” SNe Ia, produced by young ($\sim 10^8$ yr) stellar populations, while most of the SNe Ia that occur at low redshift today are “tardy”, produced by an older (several Gyrs) population. We suggest that the shallow silicon SNe Ia tend to be the prompt ones.

Subject headings: Supernovae

¹Homer L. Dodge Department of Physics and Astronomy, University of Oklahoma, Norman, OK; branch@nhn.ou.edu

²Department of Physics, University of Idaho, Moscow, ID

³Department of Physics and Astronomy, Dartmouth College, Hanover, NH

⁴Department of Physics, Stockholm University, Stockholm, Sweden

⁵Department of Physics, Worcester Polytechnic Institute, Worcester, MA

1. INTRODUCTION

This is the fourth in a series of papers on a comparative direct analysis of the optical spectra of Type Ia supernovae (SNe Ia). Paper I (Branch et al. 2005) was concerned with a time series of spectra of the spectroscopically normal SN 1994D, Paper II (Branch et al. 2006) was devoted to spectra obtained near maximum light, and Paper III (Branch et al. 2007) concentrated on premaximum spectra. This paper is about postmaximum spectra, which form in the deeper, lower velocity ejecta.

In Paper II we divided the maximum-light (B maximum) spectra into four groups: core normal, broad line, cool, and shallow silicon (denoted CN, BL, CL, and SS, respectively, in this paper). The group assignments were made on the basis of measurements of the (pseudo) equivalent widths of absorption features near 5750 and 6100 Å, as well as on the appearance (depth, width, and shape) of the 6100 Å absorption, which is produced by the Si II $\lambda 6355$ transition. Although we framed the presentation and discussion in terms of the four groups, in the end we concluded that for the most part the spectra appeared to have a continuous distribution of properties, rather than consisting of discrete subtypes (the extreme SS SN 2002cx–likes being an apparent exception, and the extreme CL SN 1991bg–likes being a possible exception). In Paper III we found that to a large extent the premaximum spectra exhibited the defining characteristics of the four groups.

In this paper, as in the previous ones, we confine our attention to optical spectra, from the Ca II H and K feature in the blue (~ 3700 Å) to the Ca II infrared triplet (Ca II IR3) in the red (~ 9000 Å). All spectra have been corrected for the redshifts of the host galaxies, and mild smoothing has been applied to some of the spectra. All spectra have been flattened according to the local normalization procedure of Jeffery et al. (2007), which eliminates all significant broad band continuum variations, including those caused by interstellar reddening and observational error. Thus the locally normalized spectra allow valid comparisons of intrinsic line features. But note that a locally normalized spectrum is not a unique representation of the line spectrum. It depends on the exact prescription of the local normalization procedure. We use exactly the same procedure for all spectra of this paper.

We examined all of the SN Ia postmaximum spectra available to us and selected three samples: a “1 week postmax” sample, consisting of one spectrum each of 21 SNe Ia observed between day +6 and day +8 with respect to the time of maximum brightness in the B band; a “3 week postmax” sample of 19 SNe Ia observed between day +19 and day +23; and a “3 months postmax” sample of 15 SNe Ia observed between day +81 and day +98 (an interval of day +80 to day +100 yielded no additional spectra). The SNe Ia and the epochs of the selected spectra are listed in Table 1. Many comparisons of subsets of these spectra have appeared in the literature. Our goal is to provide a more systematic and comprehensive

comparison.

Spectra of four of the SNe Ia of Table 1 were not available for previous papers of this series. Sadakane et al. (1996) published spectra of SN 1995D obtained shortly after maximum light, but it is difficult to decide from their Figure 3 whether SN 1995D should be assigned to the CNs or the SSs. On the basis of the report by Benetti & Mendes de Oliveira (1995) that in a 1 week premax spectrum the 5750 Å absorption was unusually weak if present at all, we tentatively assign SN 1995D to the SS group. Pastorello et al. (2007) referred to SN 2004eo as a transitional SN Ia because its properties placed it between the three groups (faint, low velocity gradient, and high velocity gradient) of Benetti et al. (2005). In our classification, the maximum light spectrum of SN 2004eo is not quite CN; it resembles that of SN 1989B (Paper II), and like SN 1989B it is placed in the CL group although it does not contain the blue “Ti II trough” of the more extreme members of the CL group. The maximum light spectrum of SN 2006X (Wang et al. 2007) is that of an extreme BL SN Ia, such as SN 1984A. Hicken et al. (2007) showed that an early spectrum of SN 2006gz had the strongest C II $\lambda 6580$ absorption yet seen in a SN Ia, and argued that super-Chandrasekhar mass ejection is required. Although no spectrum was obtained within three days of maximum light, at earlier epochs SN 2006gz showed characteristics of a SS event, and we tentatively classify it as such.

2. CALCULATIONS

Continuing our attempt to provide an internally consistent quantification of SN Ia spectra, we have used the parameterized resonance-scattering synthetic-spectrum code, SYNOW, to fit the spectra of Table 1. The excitation temperature is fixed at a nominal value of 7000 K, as was done for the postmaximum SN 1994D spectra of Paper I. A change of procedure from our previous work with SYNOW on postmaximum spectra, including that of Paper I, is that instead of using exponential (Paper I) or power-law radial optical depth distributions, we use a flat distribution with an imposed maximum velocity, v_{\max} , for every ion. In the outer layers of the ejected matter, a decreasing density is dictated by hydrodynamical models (and by mass conservation: the density must start decreasing somewhere), but in the deeper layers the density gradient is less steep. Since the optical depth distribution depends also on composition, excitation, and ionization gradients, a flat optical depth distribution is not unreasonable. For further economy of parameters, for a given spectrum we use the same value of v_{\max} for all singly ionized members of the iron group, from Sc II to Ni II (with the exception of the 1 week postmax spectrum of SN 2000cx; § 3.) The price to be paid is that the fits are not optimized, but the fitting procedure becomes more efficient (there is no need

to vary the v_e parameter) and the parameters become easier to compare: for each ion we have just a reference-line optical depth and the velocity interval in which the lines of the ion are forming in the synthetic spectrum, the minimum velocity being either the velocity at the photosphere v_{phot} or a higher detachment velocity (i.e., detached from the photosphere). Since we use only one optical depth component for each ion, in this paper it is not necessary to use the HV (high velocity) and PV (photospheric velocity) terminology of previous papers of this series.

Consider the effects, when switching from an exponential to a flat optical depth distribution, on the relative importance of lines of the same ion but of different strengths. In the flat case, the optical depths of the strongest lines need to be smaller than in the exponential case, since they maintain the same optical depths all the way to v_{max} . Lines that are somewhat weaker, but whose optical depths still remain above unity in the flat case, become relatively more important, because they now form over just as large a velocity interval as the strongest lines. Lines whose optical depths are reduced from above unity in the exponential case to well below unity in the flat case no longer conspicuously affect the spectrum.

As an example, Figure 1 compares synthetic spectra for Fe II, with flat and exponential optical depth distributions. The flat case has the parameters that we use in § 4 for the day +22 spectrum of the CN SN 1996X: $\tau(\text{Fe II})=12$, $v_{\text{phot}} = 6000 \text{ km s}^{-1}$, and $v_{\text{max}} = 13,000 \text{ km s}^{-1}$. The exponential case has the parameters that we used in Paper I for the day +24 spectrum of the CN SN 1994D: $\tau(\text{Fe II})=200$, $v_{\text{phot}} = 9000 \text{ km s}^{-1}$, and exponential e -folding velocity $v_e = 1000 \text{ km s}^{-1}$. Note that the flat case requires a lower value of v_{phot} than the exponential case. While the two synthetic spectra are similar, there are some significant differences, such as the near disappearance in the flat case of the absorption that appears near 5380 Å in the exponential case, and the higher flux peak near 4660 Å in the flat case.

3. ONE WEEK POSTMAX

One week postmax is in the middle of what we referred to in Paper I as the postmaximum “Si II phase” (from two to 12 days past maximum, for SN 1994D), because the 6100 Å absorption is deep and apparently unblended, at least in its core. At 1 week postmax the spectra are not radically different from at maximum light.

Figure 2 shows the 1 week postmax spectra of the CNs. The spectra are very similar. A log plot such as Figure 2 is convenient for comparing multiple spectra at once, but since the spectra are displaced from each other, it can be difficult to appreciate the degree of the homogeneity. Figure 3 directly compares the spectra of SN 1998bu and SN 1996X, to

show how strikingly similar these two spectra are. Even the difference at the red end of the SN 1998bu spectrum is not necessarily real, because observed spectra sometimes have problems at their ends, and also because the local normalization technique can mildly warp the ends of the spectra (Jeffery et al. 2007).

An example SYNOW fit is shown in Figure 4. The fit is to the spectrum of the CN SN 1996X (selected because it is the best spectrum of Figure 2, not because it is the best fit). The fitting parameters for SN 1996X (and other selected spectra of Figure 2) are in Table 2. Apart from the flat optical depth distribution, the fit of Figure 4 is a conventional one. The ions are the same as were used for the 1 week postmax spectrum of SN 1994D in Paper I, except that here Cr II also is included. Lines of O I, Si II, S II, Ca II, and Fe II produce most of the features in the synthetic spectrum, and we are confident that these ions are present in the observed spectrum. The presence in the observed spectrum of Na I, Mg II, Cr II, Fe III, and Co II is not definite, but we use them in the synthetic spectrum because they are plausible and they improve the fit.

The three main discrepancies in Figure 4 are familiar problems with SYNOW fits. First, for Ca II we choose parameters to fit the observed IR3 feature, because it is less blended and more sensitive to optical depth than the H and K feature; in this case, this causes the synthetic H and K absorption to be too strong. Second, the flux minimum from about 6900 to 7100 Å has no counterpart in the synthetic spectrum. The only identification that we can suggest is [O II] $\lambda\lambda 7320, 7330$, which was discussed in the context of SN 1991T by Fisher et al. (1999) and of the Type Ic SN 1994I by Millard et al. (1999). However, at later epochs this discrepancy becomes stronger, and invoking [O II] to solve it would imply excessive mass and kinetic energy of oxygen (at least for an exploding white dwarf). More likely, what we are seeing in Figure 4 is an early, mild manifestation of a discrepancy that is due to our simplifying assumption of resonant scattering. Third, the synthetic spectrum lacks absorption from about 7600 to 7800 Å. The observed absorption in this region presumably is due to Mg II $\lambda 7890$, blended with O I $\lambda 7772$, but in SYNOW spectra the synthetic absorption usually is too blue, even when Mg II is undetached, as it is here.

Most of the spectra of Figure 2 are so similar that it is not worth reporting fitting parameters for every spectrum. The exception is SN 2004S, which has much stronger high velocity Ca II absorption than the others. Krisciunas et al. (2007) termed SN 2004S a clone of SN 2001el, another CN with exceptionally strong high velocity Ca II features (Wang et al. 2003; Kasen et al. 2003; Mattila et al. 2005; Paper II). Krisciunas et al. noted that at maximum light SN 2004S had an unusually low Si II absorption blueshift for a spectrum containing the usual SN Ia features, and that the blueshift decreased more rapidly than in SN 2001el. We find that at 1 week postmax, all absorptions other than those of Ca II are

less blueshifted than in the other spectra of Figure 2; consequently our fit for SN 2004S has a low value of $v_{\text{phot}} = 7000 \text{ km s}^{-1}$ (Table 2), instead of $11,000 \text{ km s}^{-1}$ as used for the others of Figure 2.

Figure 5 shows the 1 week postmax spectra of the BLs (plus the spectrum of the CN SN 1996X for comparison). At this epoch the spectrum of SN 2002er is like that of a CN. SN 1992A retains some of its BL characteristics and remains mildly different from CN. The spectra of SN 2002bf, SN 2006X, and SN 1984A are obviously different from CN, but similar to each other. Their 6100 \AA absorptions are deeper, broader, and more blueshifted, and they have deep absorptions from about 4700 to 5100 \AA . A fit to SN 2002bf is shown in Figure 6. The 6100 \AA absorption and the deep absorption from 4700 to 5100 \AA are matched by using a high v_{max} of $21,000 \text{ km s}^{-1}$ for Si II and Fe II, compared to a typical value of $15,000 \text{ km s}^{-1}$ for the CNs at 1 week postmax. The Fe II features of SN 2005bf are so prominent that it is difficult to determine whether lines of Mg II, Fe III, and Co II are present.

The 1 week postmax spectra of the CLs are shown in Figure 7. At this epoch SN 1989B is like that of a CN and SN 2004eo is only mildly different. The spectrum of the extreme CL SN 1999by, a SN 1991bg-like (Garnavich et al. 2004), is more highly evolved than the others of the 1 week postmax sample, in fact it has more in common with the 3 week postmax spectra of the CNs than with their 1 week postmax spectra. A fit for SN 1999by is shown in Figure 8. The presence of Si II, Ca II, Ti II, and Fe II is definite, while Mg I, Sc II, and Cr II are plausible and improve the fit. There are three main discrepancies. First, the synthetic absorption near 5340 \AA , produced by Cr II, is not deep enough, even though Cr II is too strong in several other places. (A corresponding feature in the CNs of the 3 week postmax sample is discussed in § 4.) Second, the observed absorption near 5820 \AA has practically no counterpart in the synthetic spectrum. The only identification we can offer is Si II $\lambda 5972$, but it hardly appears in the synthetic spectrum even though the absorption feature of the $\lambda 6355$ Si II reference line is too strong. Third, the synthetic flux peaks near 4000 and 4600 \AA are too high; this may be a consequence of the flat optical depth distribution (see the 4600 \AA peak in Figure 1.) Our present SNOW fit differs from the one presented in Garnavich et al. in that we do not use Ca I, Ti II makes no significant contribution to the synthetic spectrum at wavelengths longer than 5300 \AA , and we do invoke Mg I, Sc II, and Cr II.

Figure 9 shows the 1 week postmax spectra of the SSs. SN 2006gz is intermediate between the CN SN 1996X and the SS SN 1999aa, which has weaker Si II, S II, and Ca II absorptions. Hicken et al. (2007) identified C II in spectra of SN 2006gz obtained 10 or more days before maximum light, after which the feature was not identifiable, consistent with the lack of evidence for C II in the spectrum shown in Figure 9. The direct comparison of SN 1999ac and SN 1996X in Figure 10 is interesting. SN 1999ac has Si II and S II

absorptions that are less blueshifted than in SN 1996X, but Fe II features from 4700 to 5100 Å that are more blueshifted. A fit for SN 1999ac is shown in Figure 11. The presence of O I, Si II, S II, Ca II, and Fe II in SN 1999ac is definite; Na I, Mg II and Fe III are plausible. To account for the above mentioned peculiarity, we use a low photospheric velocity of 6000 km s⁻¹ and a higher v_{\max} for Fe II (15,000 km s⁻¹) than for most of the other ions (see Table 2). The spectra of SN 1999ac have been discussed extensively by Garavini et al. (2005). They emphasized the unusually low Si II blueshift, consistent with our use of a low photospheric velocity. They also concluded that Fe II lines formed at unusually low velocities, but our v_{\max} of 15,000 km s⁻¹ is the same as we use for the CN SN 1996X.

The Ca II IR3 feature of SN 2000cx obviously differs from the others of Figure 9. Otherwise, the closest match to SN 2000cx is SN 1999aa, but there are conspicuous differences. The fit for SN 2000cx shown in Figure 12 is unusual because, as in Paper II, we resort to detached high-velocity Ti II, Cr II, and Fe II. In fact, in the synthetic spectrum most of the photospheric features are at least mildly detached (Table 2). Still, the fit is not very good. Although the synthetic Ca II H and K absorption is much too strong, the IR3 does not appear. The observed multicomponent absorption of the IR3 has been discussed by Li et al. (2001), Wang et al. (2003), Kasen et al. (2003), and Thomas et al. (2004), and is known to have involved asymmetrical structures at high velocity.

4. THREE WEEKS POSTMAX

Three weeks postmax is in the middle of what we referred to in Paper I as the “Si II–to–Fe II transition phase” (from 14 to 28 days past maximum, for SN 1994D) because the core of the 6100 Å absorption is present but flanked by strengthening Fe II features. The 3 week postmax spectra are very different from the 1 week postmax spectra.

Figure 13 shows the 3 week postmax spectra of the CNs, and a fit for SN 1996X is shown in Figure 14. The ions are the same as were used for SN 1994D at comparable epochs in Paper I. Apart from the Ca II and Na I features, the dominant ion is Fe II, but Si II, Cr II, and to a lesser extent Co II are also needed. Fitting parameters for SN 1996X and other selected spectra of the 3 week postmax sample are given in Table 3.

The degree of homogeneity in Figure 13 is very high, except in two respects. First, SN 2001el and SN 2004S still have strong high velocity Ca II H and K absorptions (and most of the absorption features of SN 2004S continue to be somewhat less blueshifted than in the others). Second, the relative heights of the flux peaks that flank the 5350 Å absorption are not all the same. The relative heights of these two peaks were discussed in Paper I: in

SN 1994D the ratio of the peak on the right of the 5350 Å absorption to the peak on the left increased steadily from day +15, when the peaks were roughly equally high, to day +28, when the peak on the right was much higher. Our fits accounted nicely for this evolution, in terms of strengthening Fe II and Cr II lines. In this respect, some of the spectra of Figure 13 appear to be spectroscopically “earlier” than some of the others. For example, the day +21 spectrum of SN 1998aq (Fig. 13) has equally high peaks, like the day +15 spectrum of SN 1994D (Paper I), and closely resembles that spectrum in other respects also. Even CN spectra can get mildly out of phase, with respect to the time of B-band maximum.

The 3 week postmax spectra of the BLs are shown in Figure 15. At this epoch SN 1981B is like CN and so is SN 2002er, apart from its deep high velocity Ca II H and K absorption (which is not matched by the appearance of the IR3 absorption). Even the extreme BL SN 1984A appears to differ only mildly from CN, although the limited wavelength coverage does not allow us to see how the Ca II lines are behaving.

Figure 16 shows the 3 week postmax spectra of the CLs. At this epoch SN 1989B and SN 2004eo are like CN. SN 1986G remains mildly different, e.g., its 5750 Å absorption is shallow, and the ratio of the flux peaks flanking the 5350 Å absorption is very large. SN 1991bg continues to show obvious differences. A fit for SN 1991bg is shown in Figure 17. All 7 ions used in the synthetic spectrum are considered to be definite. In the blue the synthetic spectrum is a complex blend of Ti II, Cr II, and Fe II. Not only does SN 1991bg have Ti II while CNs do not, but also Cr II plays a more important role than it does in the CNs.

The 3 week postmax spectra of the SSs are shown in Figure 18. SN 1999ee is similar to CN, although with a strong high velocity Ca II H and K absorption. SN 1999aa also is similar to CN except for the spectroscopically “early” ratio of the flux peaks flanking the 5350 Å absorption. In this respect, as in others, the day +19 spectrum of SN 1999aa in Figure 18 is a good match to the day +14 spectrum of SN 1994D (Paper I).

As shown in previous papers (Chornock et al. 2006; Phillips et al. 2007; Stanishev et al. 2007), at multiple epochs the spectra of SN 2002cx and SN 2005hk are very similar. In Figure 18, the spectra of both have been artificially blueshifted by 5000 km s^{-1} , to approximately align their absorption features with those of the other SSs. The direct comparison in Figure 19 of SN 2005hk and the CN SN 1996X shows that although the features of SN 2005hk are narrower, when the spectrum of SN 2005hk is artificially blueshifted, the features of the two spectra show a strong correspondence. Not only the absorptions but also the flux peaks match up well. If the flux peaks of SN 2005hk were true emission peaks, at the rest wavelengths of the lines that produce them, then after the blueshifting, the peaks would be bluer than those of SN 1996X. This is in accord with the maxim that in heavily

blended resonance-scattering spectra, “absorptions trump emissions”, i.e., flux peaks do not necessarily occur at the rest wavelengths of the strongest lines, because they are strongly influenced by absorption components of mainly redward lines. Figure 20 shows a fit to the (not artificially blueshifted) spectrum of SN 2005hk. The ions used are the same ones as used for the 3 week postmax spectrum of the CN SN 1996X, except that Si II is not needed for SN 2005hk. Note that it is not v_{phot} , but v_{max} for Cr II, Fe II, and Co II that differs by 5000 km s $^{-1}$ from that of SN 1996X (Table 2). Apart from the two Ca II features and the one Na I feature, the synthetic spectrum is a complex blend of Fe II, Cr II, and Co II, just as it is for SN 1996X.

As can be seen in Figure 18, at this epoch SN 2000cx remains different from CN in several ways, e.g., the peaks that appear near 4800 and 4920 Å in SN 1996X are smeared out in SN 2000cx. In this respect, SN 2000cx resembles the BL SN 2002bf of the 1 week premax sample (§ 2). To fit the spectrum of SN 2000cx we use a high maximum velocity of 18,000 km s $^{-1}$ for Fe II and Cr II (Table 2). A discussion of SYNOW fits to day +15 and +32 spectra, which have better wavelength coverage, can be found in Branch et al. (2004).

5. THREE MONTHS POSTMAX

Three months postmax is within what we referred to in Paper I as the “Fe II phase” (from 50 to 115 days after maximum for SN 1994D, with these particular limiting epochs being determined by the availability of spectra) because the 6100 Å absorption is nearly gone at 50 days and the spectrum is mainly shaped by Fe II lines. The 3 months postmax spectra are quite different from the 3 weeks postmax spectra. The spectra of the five CNs (Fig. 21) are very much alike. It is often assumed that at this epoch the spectrum is composed of optically thin, collisionally excited forbidden lines, but the SYNOW fit for SN 2003du in Figure 22 is good enough to firmly establish that whatever the underlying source of the emission, permitted lines of Na I, Ca II, and Fe II are mainly responsible for shaping the spectrum (see also the discussion in Paper I). However, our fit is very poor from 6600 to 7800 Å. It may be that the broad flux minimum near 6750 Å is not an absorption feature, and that the flux peaks from 7270 to 7700 are produced by strong net emission. Bowers et al. (1997) modeled the day +95 optical spectrum (along with the day 92 infrared spectrum) of SN 1995D assuming that the spectrum consists only of forbidden-line emissions. Their identifications of the flux peaks are shown in Figure 22 (SN 1995D and SN 2003du have the same peaks, and for some of the peaks Bowers et al. did not suggest identifications). In the blue, the Bowers et al. fit was not successful. However, our poor fit from 6600 to 7800 Å may signal that in this wavelength range forbidden emission lines are emerging without strong

modification by permitted-line scattering. On the other hand, if we make the Fe II lines stronger, thereby making our fit worse in the blue, we do begin to obtain a better fit in the 6600 to 7800 Å interval. This could be a consequence of a wavelength dependent variation in the depth of the photosphere. At present, line identifications in this wavelength range are uncertain.

At this epoch the four BL events of the 3 months postmax sample (Fig. 23), including the extreme BL SN 2006X, are similar to CN.

Among the CLs (Fig. 24), SN 1989B is like CN, SN 1986G differs mildly, and the extreme CL SN 1991bg remains distinctly different. The fit for SN 1991bg in Figure 25 shows that permitted-line scattering, mainly by Fe II, shapes the spectrum in the blue, but the fit fails from 6000 to 8000 Å. The only clear evidence for forbidden lines is the strong emission near 7250 Å, due to [Ca II] (Filippenko et al. 1992a).

At this epoch the probable SS SN 1995D and the extreme SS SN 1991T (Fig. 26) are like CN, and even the maverick SN 2000cx is only mildly different.

6. DISCUSSION

The spectra that appear in this series of papers are simply the good spectra that are available to us, so the samples are affected not only by observational bias in favor of supernovae that are bright and have slowly declining light curves, but also by the observer bias in favor of obtaining and publishing spectra of unusual events. Nevertheless, these samples clearly indicate a trend toward increasing spectroscopic conformity at later epochs. Among the 24 SNe Ia of the maximum light sample (Paper II), only 7 were admitted to the (by construction) highly homogeneous CN group. By contrast, of the 12 SNe Ia of the 3 months postmax sample, only SN 1991bg is distinctly different from the CNs. (SN 2002cx-likes would be different too, if they were in the sample.) This spectroscopic convergence suggests that although the outer layers of SNe Ia are diverse in various ways, the deep layers of most SNe Ia are fundamentally the same.

In this paper, the line identifications for the CNs are much like they were in Paper I for SN 1994D, although the fitting parameters are different because of our present use of flat optical depth distributions. The conclusion that permitted lines strongly affect the spectrum as late as 3 months postmax leads to a caveat to the statement above that the deep layers of most SNe Ia are fundamentally the same: at three months postmax the strongest permitted lines are strong, which entails line profile saturation and a limited sensitivity of the spectra to physical differences in the ejecta. If the spectra of the 3 months postmax

sample consisted simply of optically thin forbidden emission lines, saturation would not be an issue and the observed spectroscopic homogeneity would imply a startling (unbelievable?) degree of physical homogeneity. The degree of diversity should increase at still later times as the permitted lines weaken and the forbidden lines emerge unscathed. The transition from resonance-scattering to forbidden-line dominated spectra will be the subject of a future paper.

As in previous papers of this series, we find that the BL SNe Ia have essentially the same line identifications as the CNs, but with more line optical depth at high velocities. The distinct characteristics of the extreme BL events SN 1984A, SN 2002bf, and SN 2006X at 1 week postmax raises the issue of whether they are a discrete subgroup, but only in terms of the properties of their outer layers. There is no evidence that their deep layers are unusual: by 3 months postmax, SN 2006X was like a CN.

The spectrum of the extreme CL SN 1991bg has been thought to have undergone an early transition to the nebular phase (Filippenko et al. 1992a; Leibundgut et al. 1993; Turatto et al. 1996; Mazzali et al. 1997). According to our interpretation (Fig. 17) there is no need to appeal to forbidden lines in the 3 week postmax spectrum (Fig. 17), and even in the 3 month postmax spectrum the only obvious one is $[\text{Ca II}] \lambda\lambda 7291, 7324$. In spite of its peculiarities, the spectrum of SN 1991bg does increasingly resemble the spectra of other SNe Ia after maximum light, and in all respects SN 1986G appears to be a link between SN 1991bg-likes and normal SNe Ia. As discussed in Paper I, the spectroscopic peculiarities of SN 1991bg-likes may largely (but not entirely) reflect a temperature threshold below which key ionization ratios change abruptly. The issue of whether SN 1991bg-likes are a distinct subgroup remains open.

The 1 week and 3 week postmax spectra of the SS SN 2000cx are unique among SNe Ia observed so far. Our identifications of high velocity Ti II and especially Cr II are not definite, but for nonstandard spectra, nonstandard identifications are to be expected, and no alternative identifications have been suggested. The resemblance of the 3 months postmax spectrum of SN 2000cx to CNs suggests, though, that its deeper layers are like those of other SNe Ia. The SN 2002cx-likes, on the other hand, appear to be radically different from other SNe Ia, even in their deeper layers. Pending the discovery of SNe Ia having less mild SN 2002cx-like properties, the SN 2002cx-likes appear to be a discrete subgroup. Yet the resemblance of their spectra, when artificially blueshifted, to other SNe Ia (Fig. 19) suggests kinship.¹

¹An anonymous referee points out that another possible discrete subgroup could be SNe Ia that have very slow light curve decline rates, such as SN 2001ay (Howell & Nugent 2004), SN 2003fg (Howell et al.

Although this series of papers is confined to spectroscopy, it is worth emphasizing that the spectroscopic diversity is bound to contribute to the photometric diversity. Branch et al. (2004) discussed the effects of the putative high velocity Ti II of SN 2000cx on the evolution of its $B - V$ color. Another good example is the 1 week postmax spectra of the extreme BLs SN 2002bf, SN 1984A, and SN 2006X (Figures 5 and 6). The deep Fe II absorption from 4700 to 5100 Å, near the intersection of the B and V bands, throws flux right into the peak of the V band (thus obscuring the S II absorptions) and is bound to affect the B-V color evolution, with implications for attempts to estimate the interstellar extinction on the basis of broad band photometry (e.g., Wang et al. 2007 for SN 2006X).

In recent years it has been shown (Mannucci et al. 2005, 2006; Scannapieco & Bildsten 2005; Sullivan et al. 2006) that some SNe Ia, called prompt, are produced by a young ($\sim 10^8$ yr) stellar population while others, called tardy, are produced by an older population (several Gyr). Most the SNe Ia that have ever occurred were prompt, but at the present epoch most of the SNe Ia at low redshift are tardy. This raises the question of which of our spectroscopic groups are prompt and which are tardy. Since the extreme CL events such as SN 1991bg tend to occur in old populations and the extreme SS events such as SN 1991T tend to occur in young populations (Sullivan et al. 2006 and references therein), if we are to break our groups into a minority of prompts and a majority of tardies, then the members of the SS group should tend to be prompts and the members of the other three groups tend to be tardies. Yet there is no obvious spectroscopic separation between the SS group and the CN group. The CN group was defined to emphasize the strong spectroscopic homogeneity of its members, but several of the SSs (e.g., SN 1999ee, SN 1999ac, SN 1999aa) are not very different from CN. As discussed in Paper II, it may be that there are two evolutionary paths to SNe Ia that require different amounts of time but produce two families of SNe Ia that have overlapping distributions of their properties.

That being said, Quimby et al. (2007) suggested that even among normal SNe Ia (in the broad sense of the term) there may be two distinct classes of events: those that have a smoothly declining density distribution in their outer layers and therefore show a blueshift of the 6100 Å absorption that decreases smoothly with time, and those in which silicon is largely confined to a shell-like density structure and therefore have a more constant blueshift of the 6100 Å absorption. The smooth density structure is characteristic of deflagration and delayed detonation models, while a shell is characteristic of pulsating delayed detonation and tamped detonation models. The suggestion of Quimby et al. was motivated by a prolonged

2006), and SN 2006gz (Hicken et al. 2007). Subclassifying SNe Ia by means of photometric characteristics is beyond the scope of this paper, but we note that in our spectroscopic classification scheme, SN 2001ay is broad line (Paper II) while SN 2003fg (Paper III) and SN 2006gz (this paper) are shallow silicon.

period of nearly constant blueshift in SN 2005hj, but they point out that some other SNe Ia such as SN 1999aa and SN 2000cx are similar in this respect. In our classification, these three events are SS. More well observed SS and CN SNe Ia are needed to determine whether SS and CN SNe Ia are distinctly different in this respect.

SYNOW is useful for establishing line identifications and information on the velocity intervals in which the lines are forming, but it is no substitute for detailed calculations of spectra of hydrodynamical models. At present no 1D explosion model has been shown to account well for the observed spectral evolution, not even for the CNs (Baron et al. 2006). Spectropolarimetry and explosion modeling tells us that asymmetries are present, but the spectra of 3D explosion models cannot yet even be calculated in full detail (although a start has been made by calculating the spectra of 3D models for angle averaged compositions; Baron et al. 2007). The homogeneity of the CNs shows that there is a standard, repeatable SN Ia explosion model that does not have large compositional inhomogeneities near or below the maximum photospheric velocity of about $12,000 \text{ km s}^{-1}$ — but what is this model? And there are many additional questions, such as: what variation on the CN model is responsible for the extra high velocity matter in the BLs, and the putative bizarre high velocity features of SN 2000cx, and the distinctive properties of the SN 2002cx-likes? We have hardly begun on the path toward understanding the various manifestations of spectroscopic diversity of SNe Ia.

We are grateful to all observers who have provided spectra. This work has been supported by NSF grants AST 0506028 and AST 0707704, NASA LTSA grant NNG04GD36G, and DOE grant DEFG02-07ER41517.

REFERENCES

Barbon, R., Iijima, T., & Rosino, L. 1989, A&A, 220, 83

Baron, E., Bongard, S., Branch, D., & Hauschildt, P. H. 2006, ApJ, 645, 480

Baron, E., Jeffery, D. J., & Branch, D., Bravo, E., Garcia-Senz, D., & Hauschildt, P. H., 2007, ApJ, in press (arXiv:0709.4177)

Benetti, S., & Mendes de Oliveira, C. 1995, IAU Circ. No. 6135

Benetti, S., et al. 2004, MNRAS, 348, 261

Benetti, S., et al. 2005, ApJ, 623, 1011

Bowers, E., et al. 1997, MNRAS, 290, 663

Branch, D., et al. 1983, ApJ, 270, 123

Branch, D., Baron, E., Hall, N., Melakayil, M., & Parrent, J. 2005, PASP, 117, 545 (Paper I)

Branch, D., et al. 2003, AJ, 126, 1489

—. 2004, PASP, 116, 903

—. 2006, PASP, 118, 560 (Paper II)

—. 2007, PASP, 119, 709 (Paper III)

Chornock, D., Filippenko, A. V., Branch, D., Foley, R. J., Jha, S., & Li, W. 2006, PASP, 118, 722

Cristiani, S., et al. 1992, A&A, 259, 63

Elias-Rosa, N., et al. 2006, MNRAS, 369, 1880

Filippenko, A. V., et al. 1992a, AJ, 104, 1543

Filippenko, A. V. 1997, in Proc. NATO Advanced Study Institute, Thermonuclear Supernovae, ed. P. Ruiz-Lapuente, R. Canal, & J. Isern (Dordrecht: Kluwer), 1

Fisher, A., Branch, D., Hatano, K., & Baron, E. 1999, MNRAS, 304, 67

Garavini, G., et al. 2004, AJ, 128, 387

—. 2005, AJ, 130, 2278

Garnavich, P. M., et al. 2004, ApJ, 613, 1120

Gomez, G., & Lopez, R. 1998, AJ, 115, 1096

Hamuy, M., et al. 2002, AJ, 124, 417

Hicken, M., Garnavich, P. M., Prieto, J. L., Blondin, S., DePoy, D. L., Kirshner, R. P., & Parrent, J., ApJ, 669, 17

Howell, D. A., & Nugent, P. 2004, in *Cosmic Explosions in Three Dimensions*, eds. P. Höflich, P. Kumar, & J. C. Wheeler (Cambridge, CUP), p. 151

Howell, D. A., et al. 2006, *Nature*, 443, 308

Jeffery, D. J., Ketchum, W., Branch, D., Baron, E., Elmhamdi, A., & Danziger, I. J. 2007, *ApJS*, 171, 493

Jha, S., et al. 1999, *ApJS*, 125, 73

Kasen, D., et al. 2003, *ApJ*, 593, 788

Kirshner, R. P., et al. 1993, 415, 589

Kotak, R., et al. 2006, *A&A*, 436, 1021

Krisciunas, K., et al. 2007, *AJ*, 133, 58

Leibundgut, B., et al. 1993, *AJ*, 105, 301

Leonard, D. C., Li, W., Filippenko, A. V., Foley, R. J., & Chornock, R. 2005, *ApJ*, 632, 450

Li, W., et al. 1999, *AJ*, 117, 2709

—. 2001, *PASP*, 113, 1178

—. 2003, *PASP*, 115, 453

Mannucci, F., Della Valle, M., & Panagia, N. 2006, *MNRAS*, 370, 773

Mannucci, F., et al. 2005, *A&A*, 433, 807

Mattila, S., et al. 2005, *A&A*, 443, 649

Mazzali, P. A., et al. 1997, *MNRAS*, 284, 151

Millard, J., et al. 1999, *ApJ*, 527, 746

Pastorello et al. 2007, *MNRAS*, 377, 1531

Patat, F., et al. 1996, *MNRAS*, 278, 111

Phillips, M. M., et al. 2007, *PASP*, 119, 360

Quimby, R., Höflich, P., & Wheeler, J. C., *ApJ*, 666, 1083

Sadakane, K., et al. 1996, *PASJ*, 48, 51

Salvo, M. E., Cappellaro, E., Mazzali, P. A., Benetti, S., Danziger, I. J., Pata, F., & Turatto, M. 2001, *MNRAS*, 321, 254

Scannapieco, E., & Bildsten, L. 2005, *ApJ*, 629, L85

Stanishev, V., et al. 2007, in preparation

Sullivan, M., et al. 2006, *ApJ*, 648, 868

Thomas, R. C., Branch, D., Baron, E., Nomoto, K., Li, W., & Filippenko, A. V. 2004, ApJ, 601, 1019

Turatto, M., et al. 1996, MNRAS, 283, 1

Wang, L., et al. 2003, ApJ, 591, 1110

Wang, X., et al. 2007, ApJ, in press (arXiv:0708.0140)

Wells, L. A., et al. 1994, AJ, 108, 2233

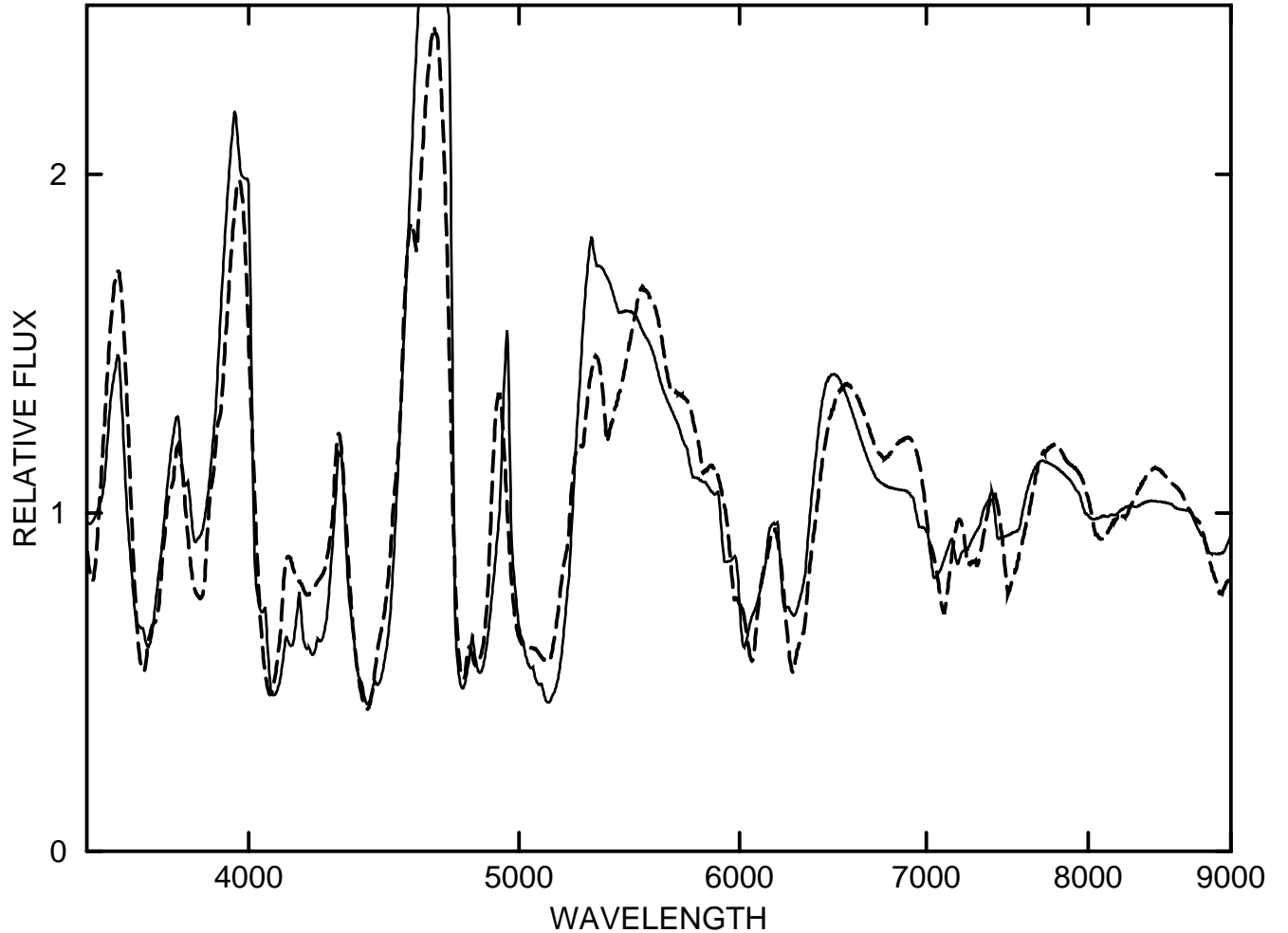


Fig. 1.— Synthetic spectra for Fe II with flat (solid line) and exponential (dashed line) optical depth distributions are compared. The parameters for the flat case are $\tau(\text{Fe II})=12$, $v_{\text{phot}} = 6000 \text{ km s}^{-1}$, and $v_{\text{max}} = 13,000 \text{ km s}^{-1}$. For the exponential case they are $\tau(\text{Fe II})=200$, $v_{\text{phot}} = 9000 \text{ km s}^{-1}$, and $v_e = 1000 \text{ km s}^{-1}$.

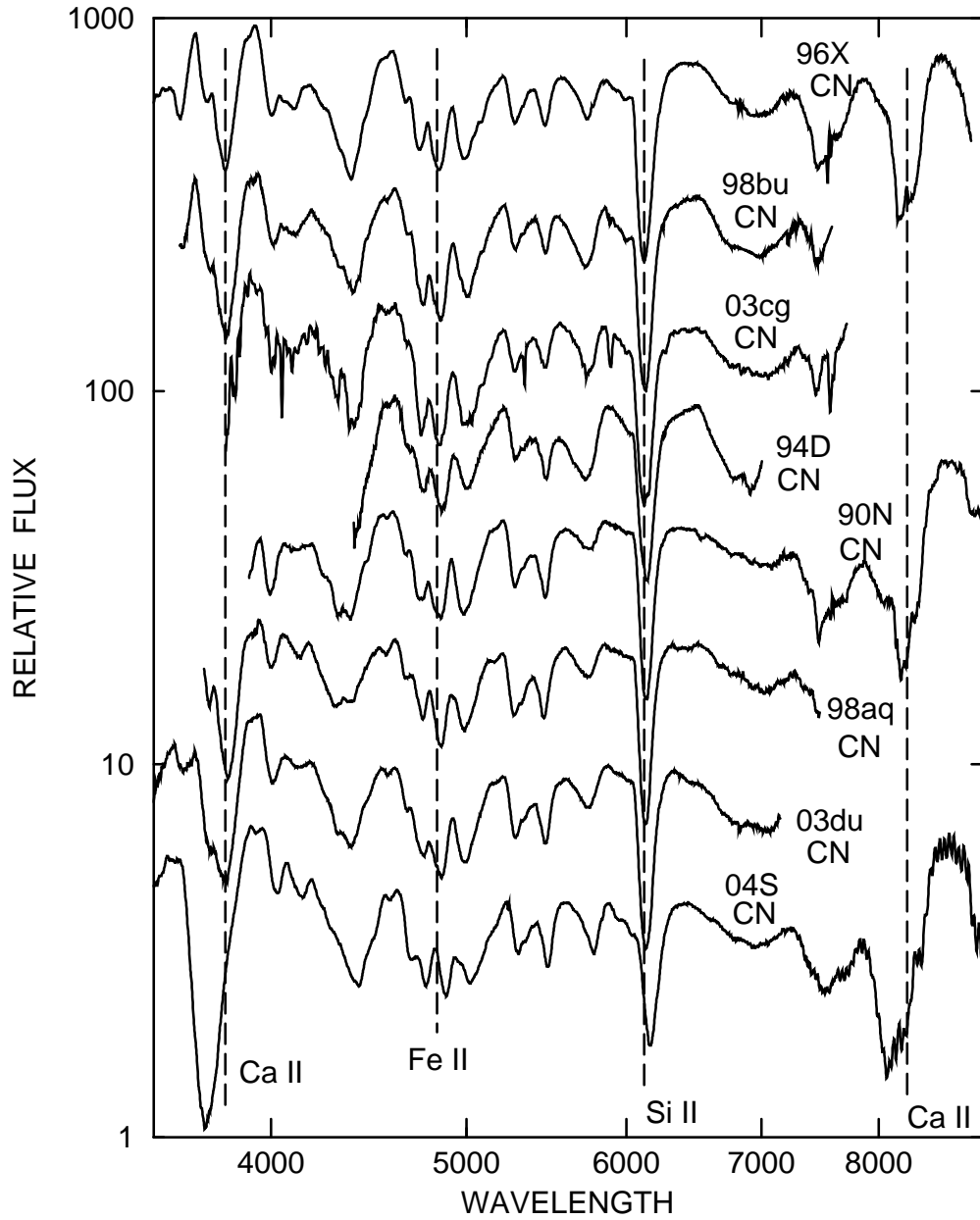


Fig. 2.— Spectra of the eight CNs of the 1 week postmax sample. The spectra have been flattened according to the local normalization technique of Jeffery et al. (2007). Vertical displacements are arbitrary and narrow absorptions near 7600 Å and 6900 Å are telluric. Vertical dashed lines refer to Ca II λ 3945, Fe II λ 5018, Si II λ 6355, and Ca II λ 8579, blueshifted by 11,000 km s⁻¹.

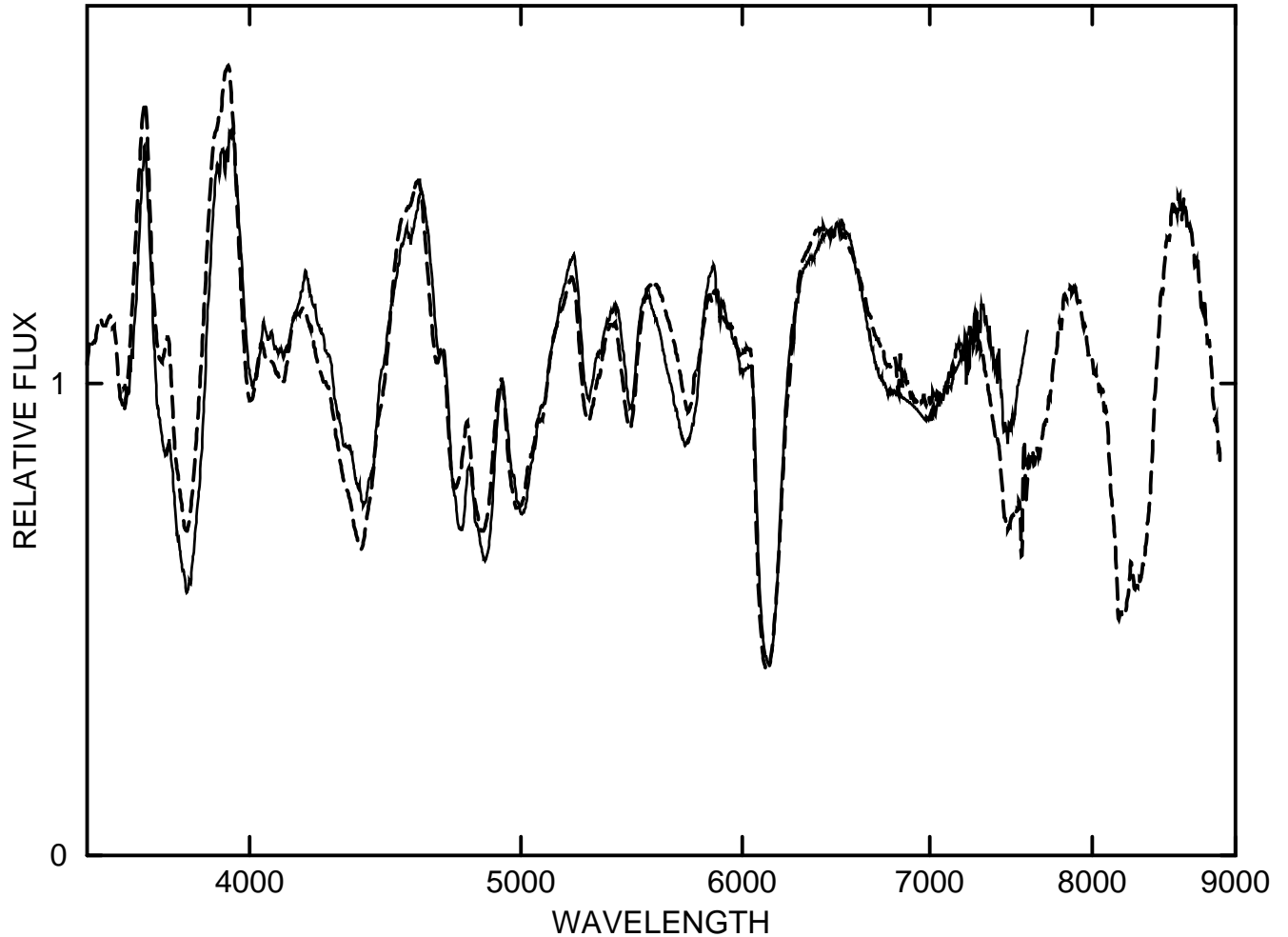


Fig. 3.— The 1 week–postmax spectra of the CN SN 1998bu (*solid line*) from Jha et al. (1999) and the CN SN 1996X (*dashed line*) from Salvo et al. (2001) are compared.

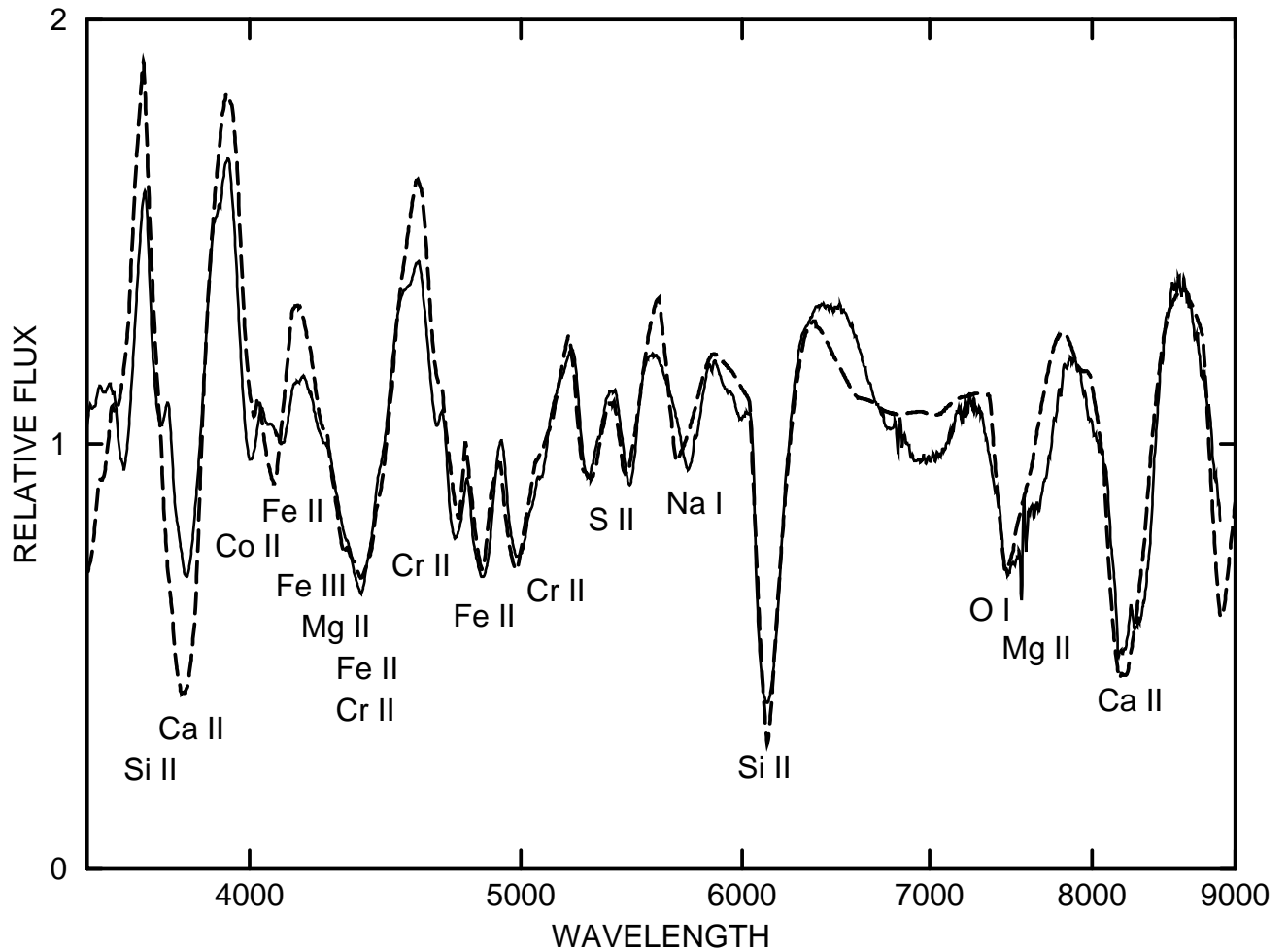


Fig. 4.— The 1 week postmax spectrum of the CN SN 1996X (*solid line*) from Salvo et al. (2001) compared with a synthetic spectrum (*dashed line*).

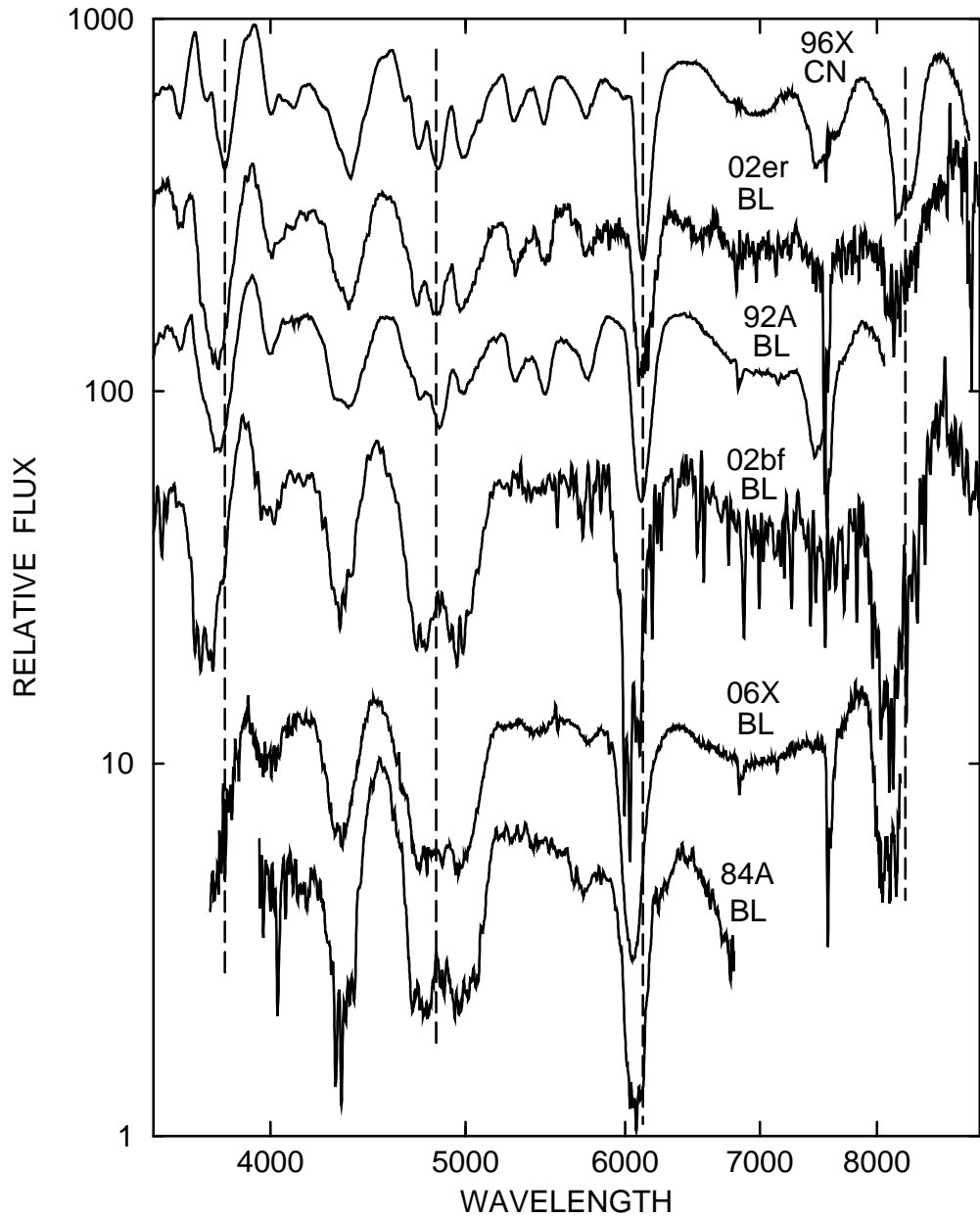


Fig. 5.— Like Fig. 2 but for one CN (for comparison) and the five BLs of the 1 week postmax sample.

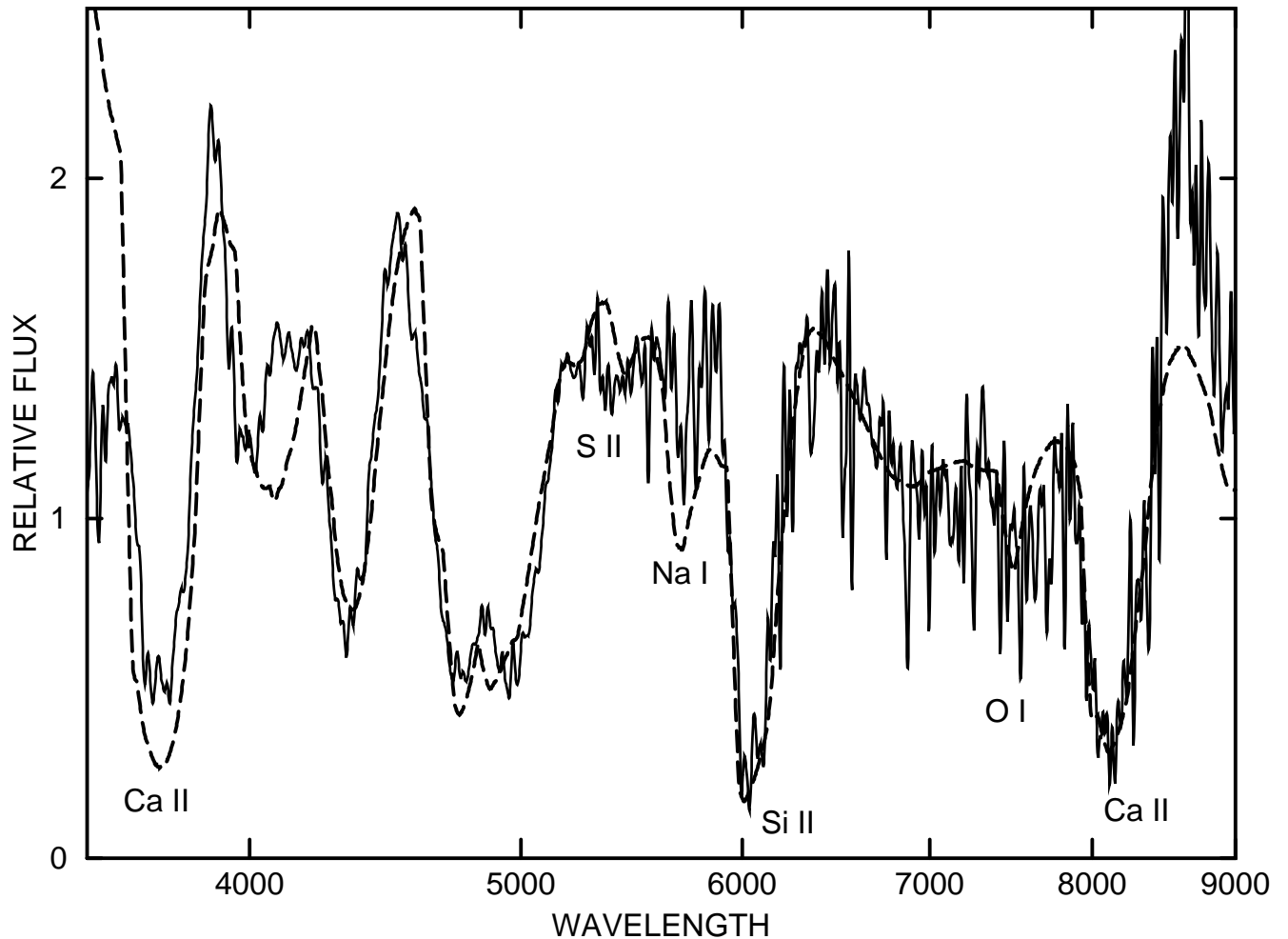


Fig. 6.— The 1 week postmax spectrum of the BL SN 2002bf (solid line) from Leonard et al. (2005) compared with a synthetic spectrum (dashed line). Unlabelled absorption features in the synthetic spectrum are produced by Fe II.

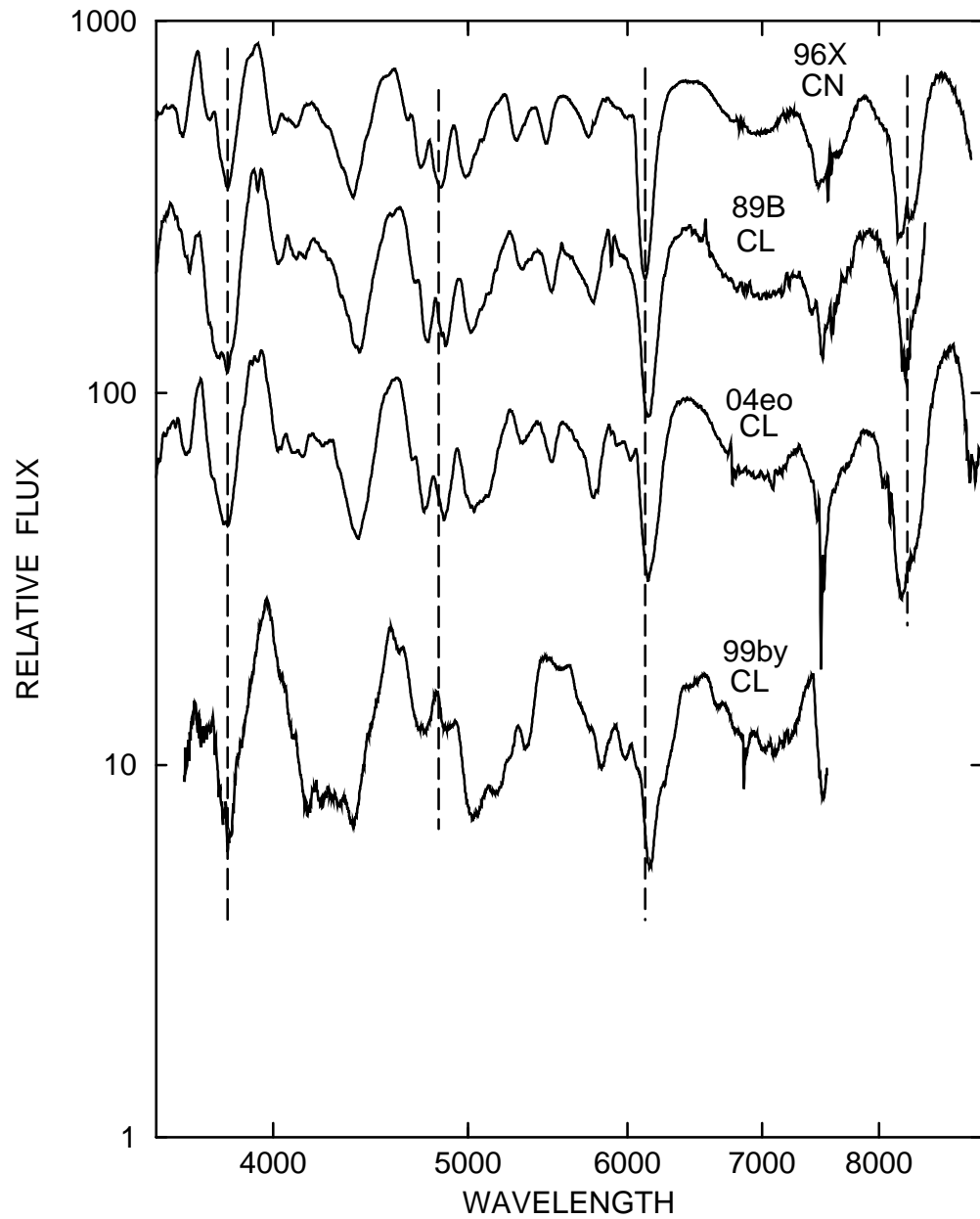


Fig. 7.— Like Fig. 2 but for one CN and the three CLs of the 1 week postmax sample.

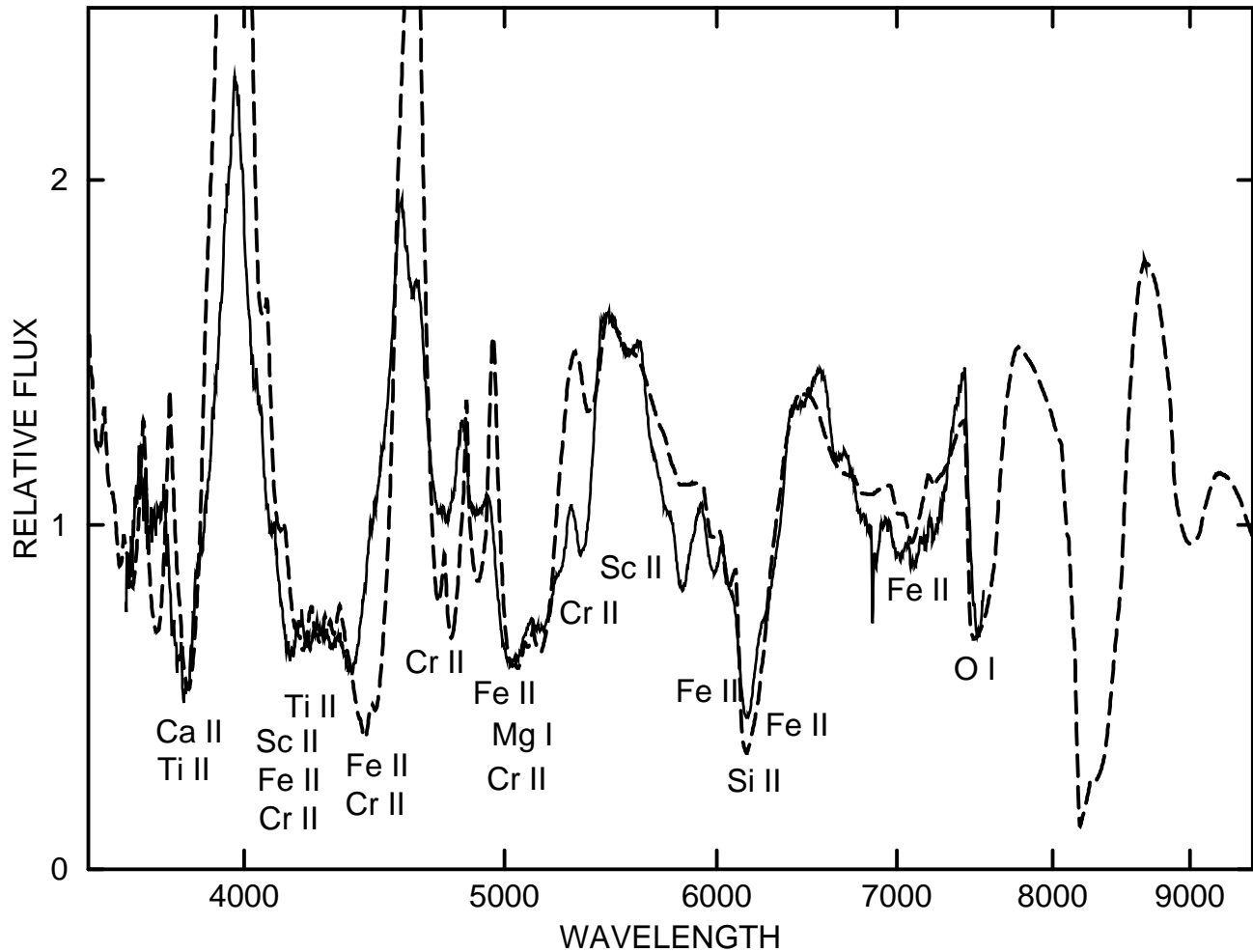


Fig. 8.— The 1 week–postmax spectrum of the CL SN 1999by (solid line) from Garnavich et al. (2004) compared with a synthetic spectrum (dashed line).

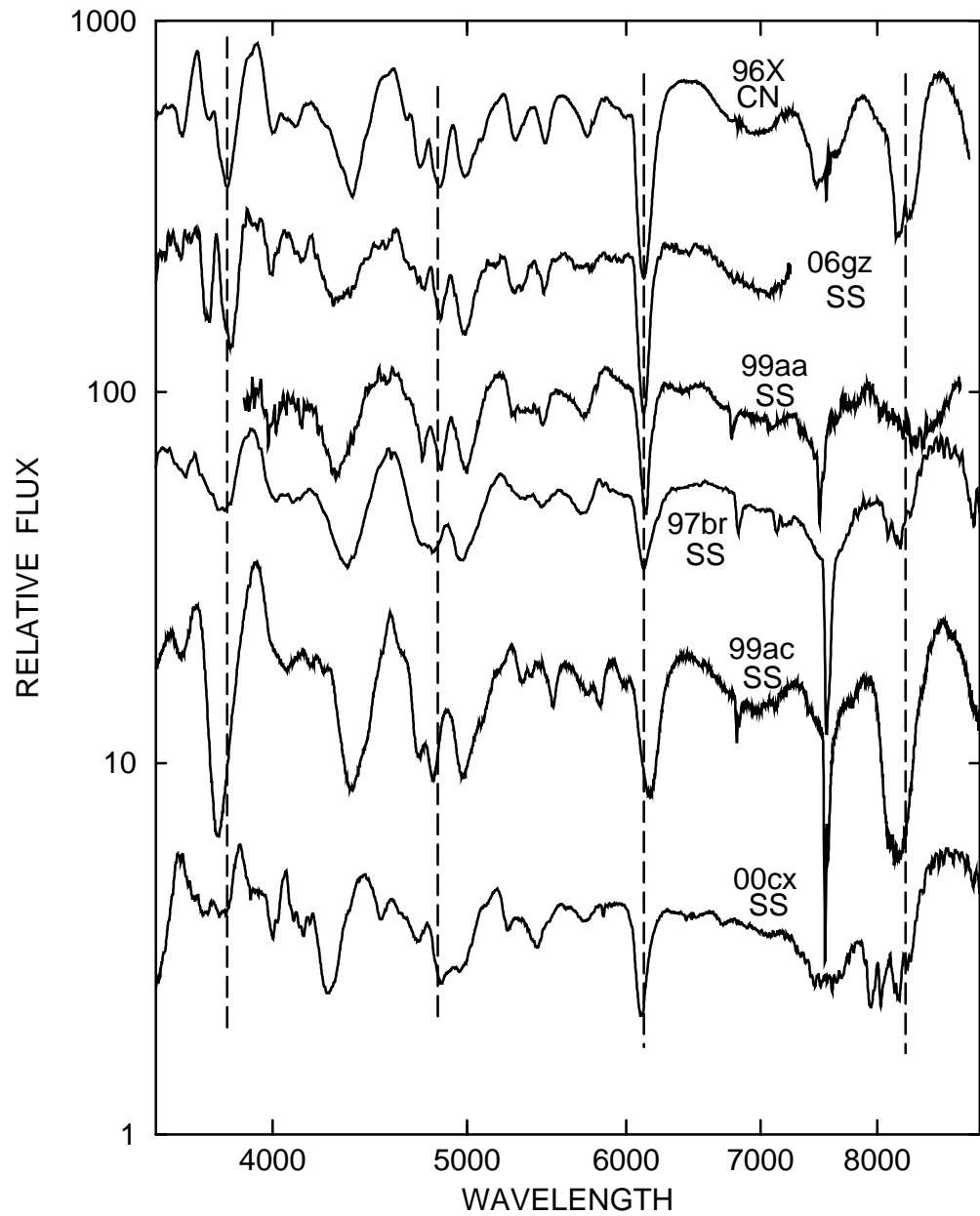


Fig. 9.— Like Fig. 2 but for one CN and the five SSs of the 1 week postmax sample.

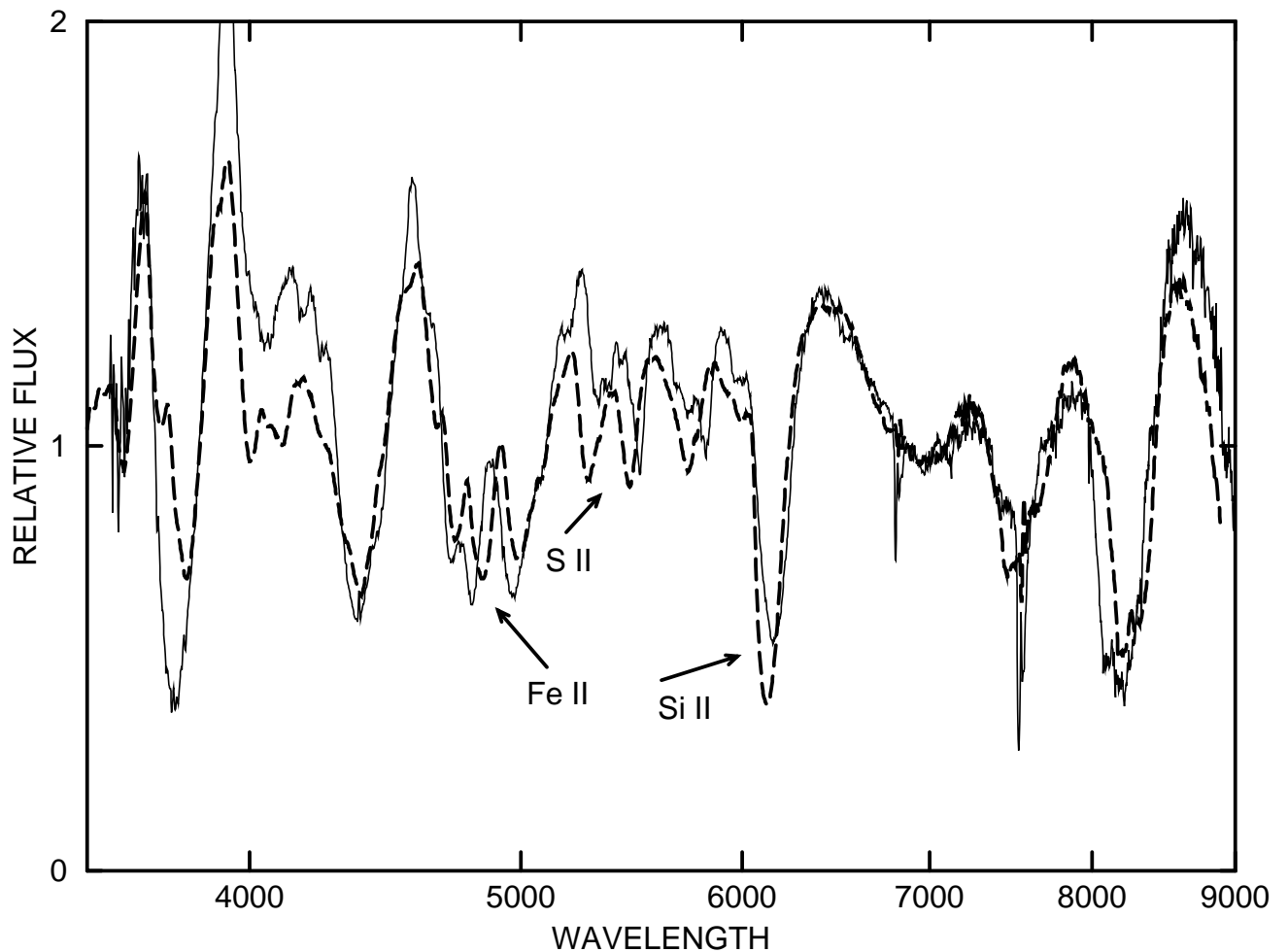


Fig. 10.— The 1 week postmax spectra of the SS SN 1999ac (solid line) from Garavini et al. (2005) and the CN SN 1996X (dashed line) from Salvo et al. (2001) are compared. The arrows point to the lower blueshifts of Si II and S II and the higher blueshifts of Fe II, in SN 1999ac.

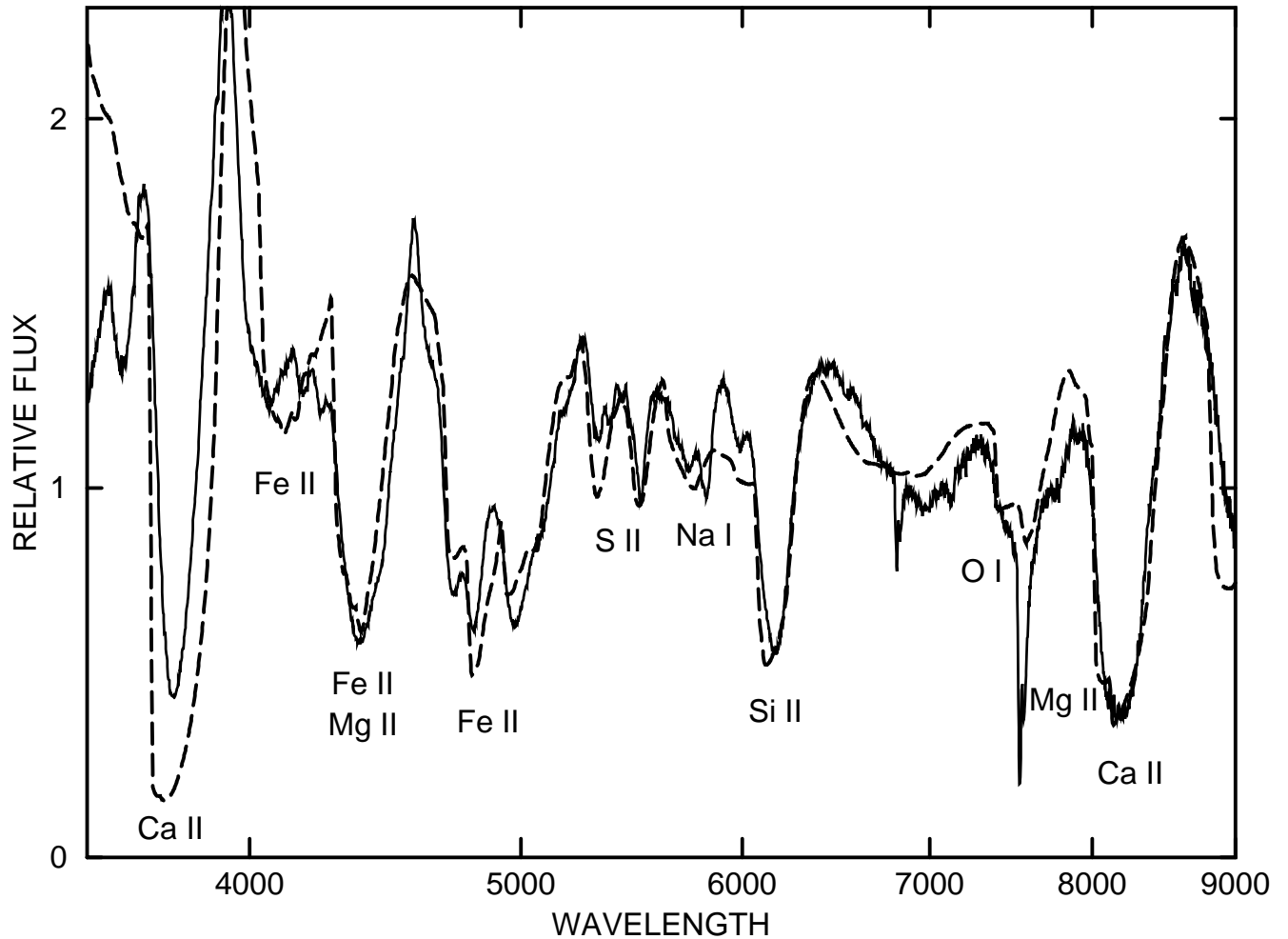


Fig. 11.— The 1 week postmax spectrum of the SS SN 1999ac (solid line) from Garavini et al. (2005) compared with a synthetic spectrum (dashed line).

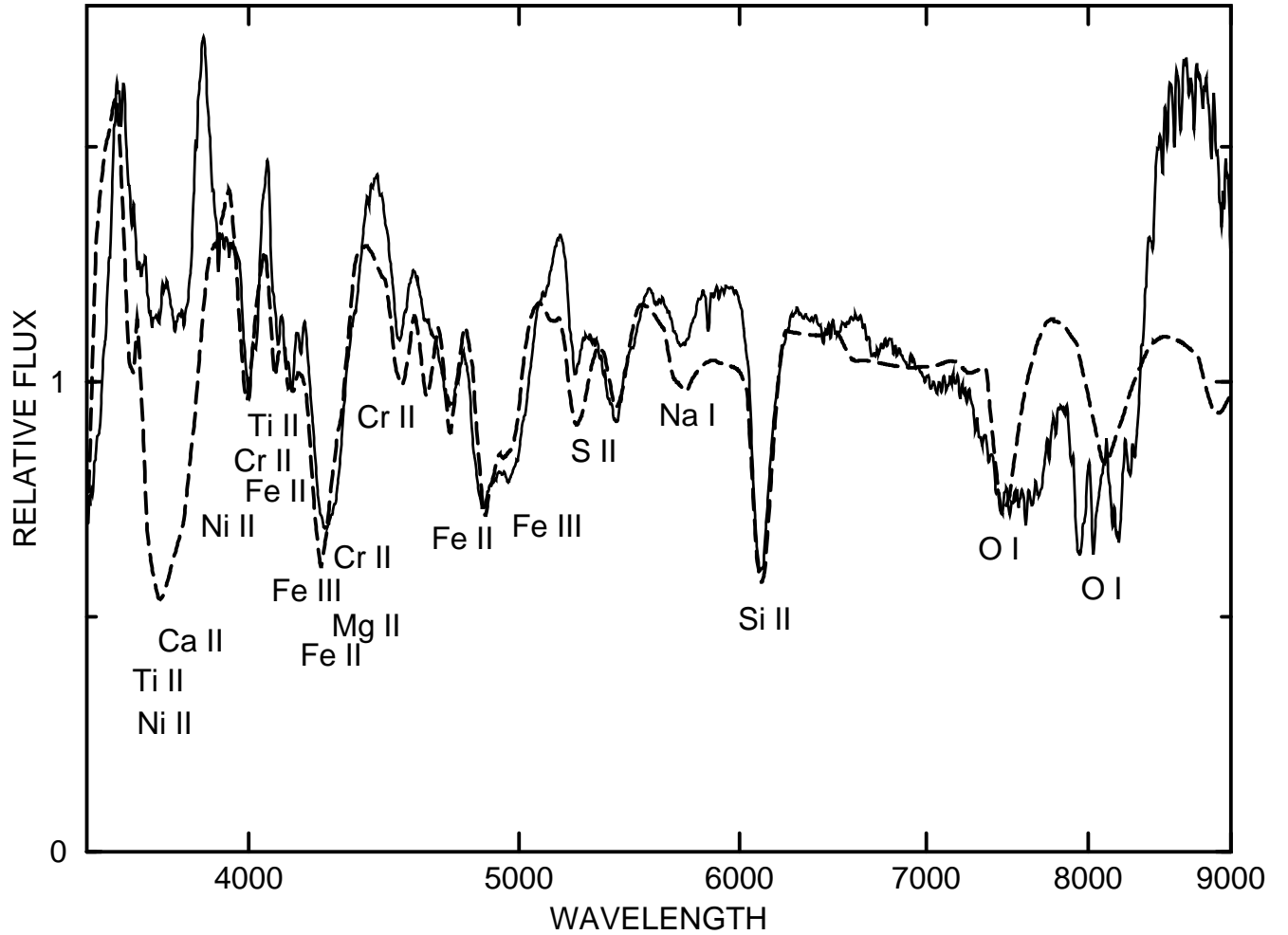


Fig. 12.— The 1 week postmax spectrum of the SS SN 2000cx (solid line) from Li et al. (2001) compared with a synthetic spectrum (dashed line). The synthetic absorption near 8000 Å is produced by O I λ 8446 but the neighboring observed absorptions are produced by the Ca II IR3.

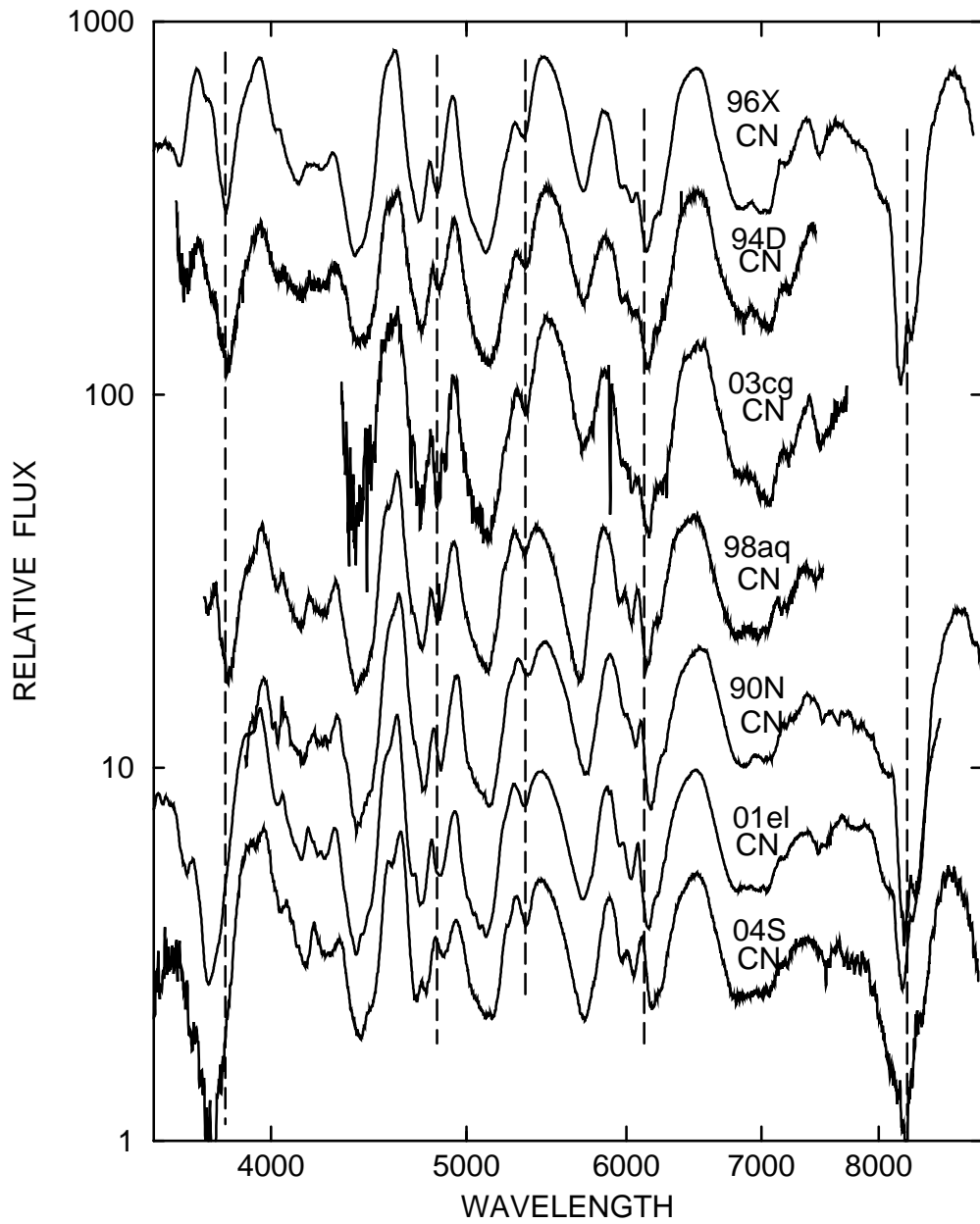


Fig. 13.— Like Fig. 2 but for the seven CNs of the 3 week postmax sample, with an additional dashed line at 5350 Å.

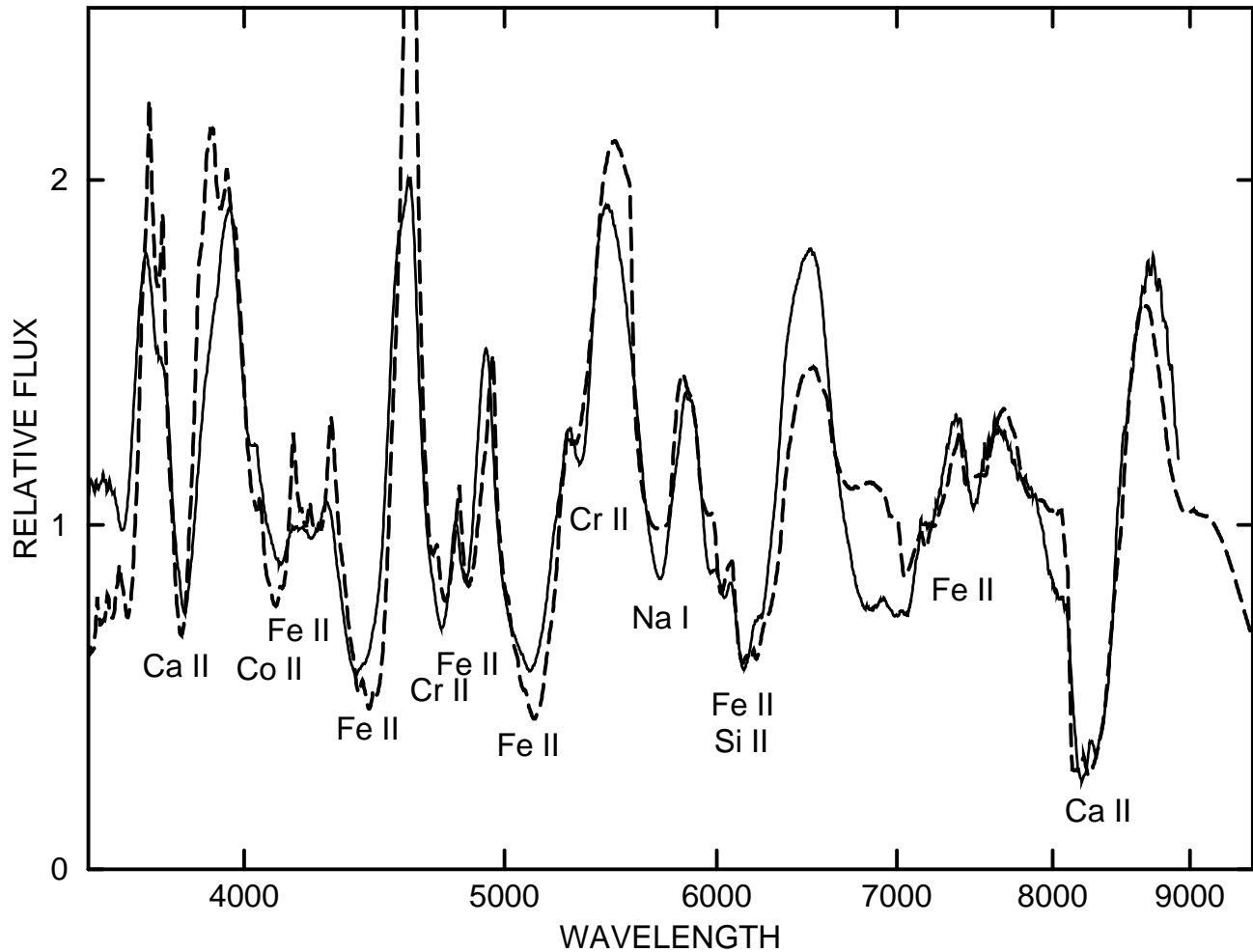


Fig. 14.— The 3 week–postmax spectrum of the CN SN 1996X (*solid line*) from Salvo et al. (2001) compared with a synthetic spectrum (*dashed line*).

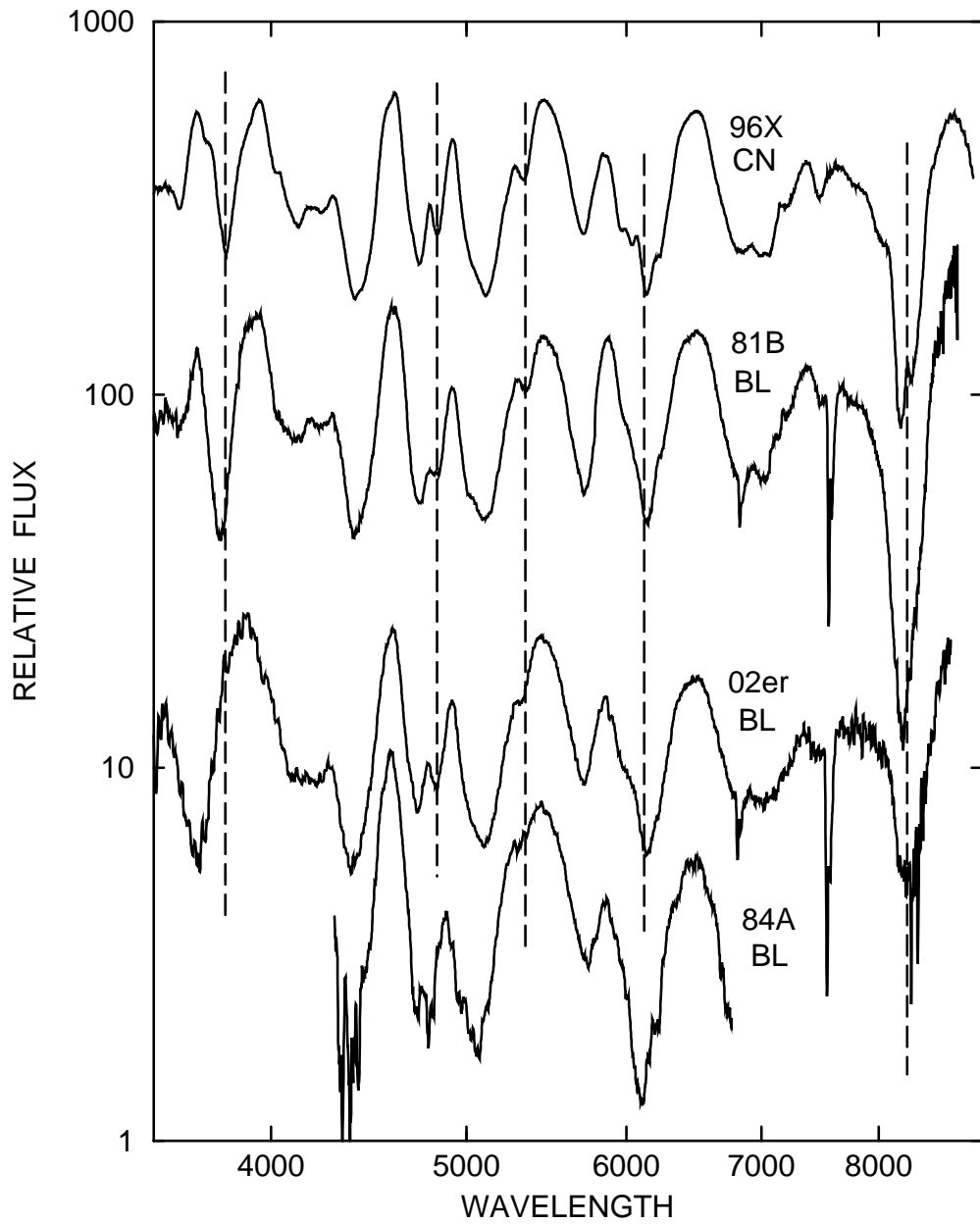


Fig. 15.— Like Fig. 2 but for one CN and the three BLs of the 3 week postmax sample, with an additional dashed line at 5350 Å.

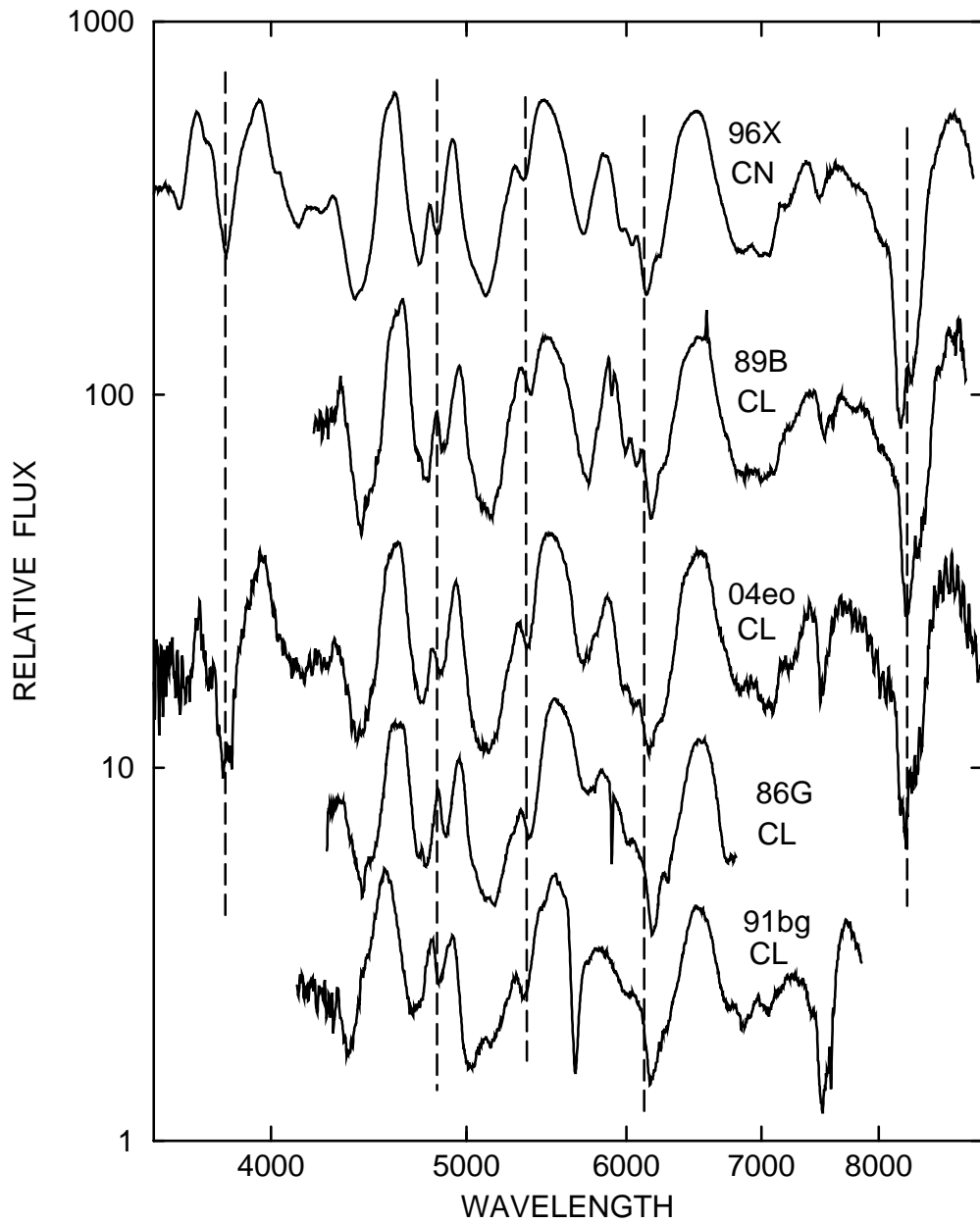


Fig. 16.— Like Fig. 2 but for one CN and the four CLs of the 3 week postmax sample, with an additional dashed line at 5350 Å.

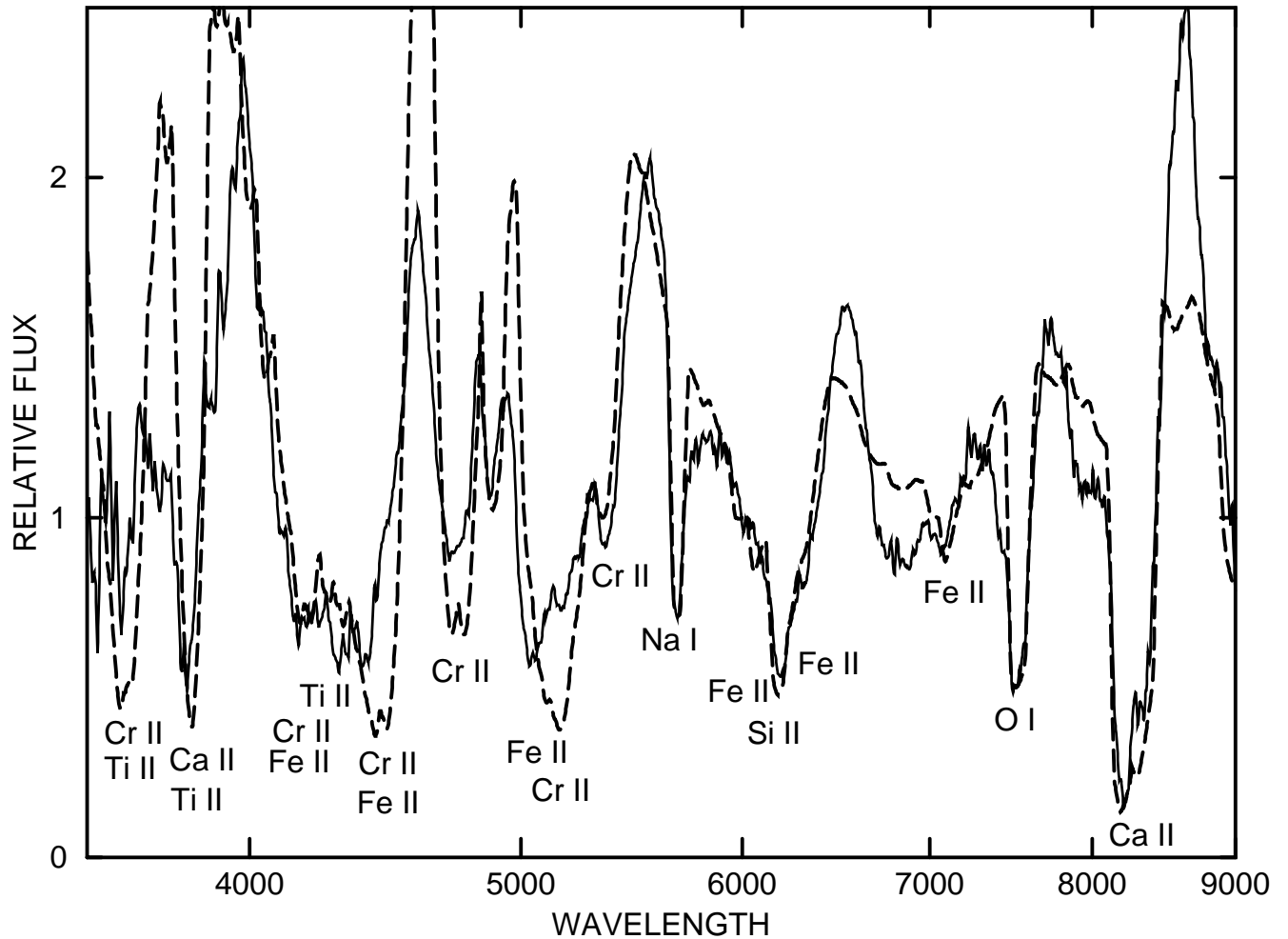


Fig. 17.— The 3 week–postmax spectrum of the CL SN 1991bg (solid line) from Filippenko et al. (1992a) compared with a synthetic spectrum (dashed line).

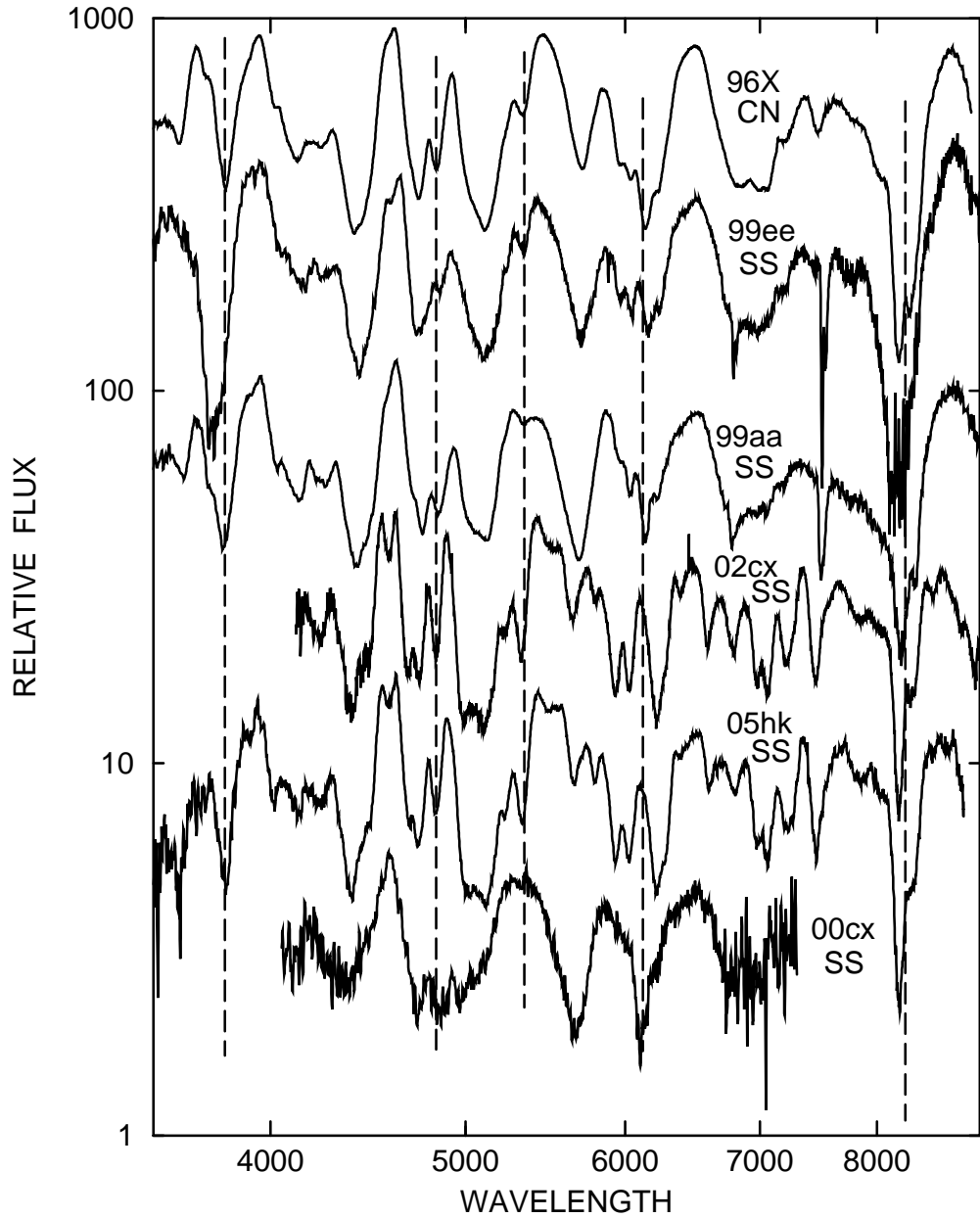


Fig. 18.— Like Fig. 2 but for one CN and the five SSs of the 3 week postmax sample, with an additional dashed line at 5350 Å. The spectra of SN 2002cx and SN 2005hk have been artificially blueshifted by 5000 km s^{−1}.

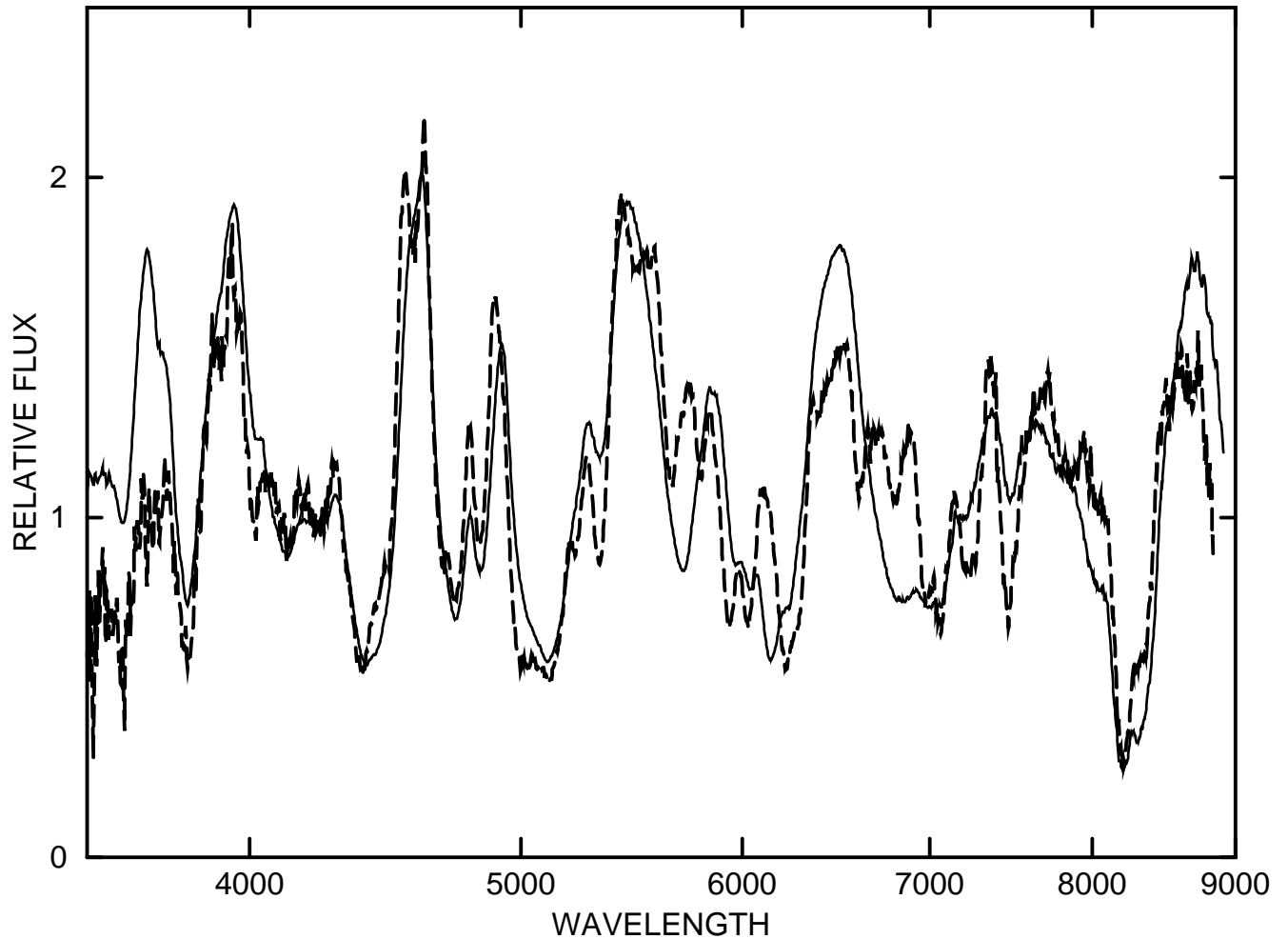


Fig. 19.— The 3 week–postmax spectra of the SS SN 2005hk (solid line) from Stanishev et al. (2007) but artificially blueshifted by 5000 km s^{-1} , and the CN SN 1996X (dashed line) from Salvo et al. (2001) are compared.

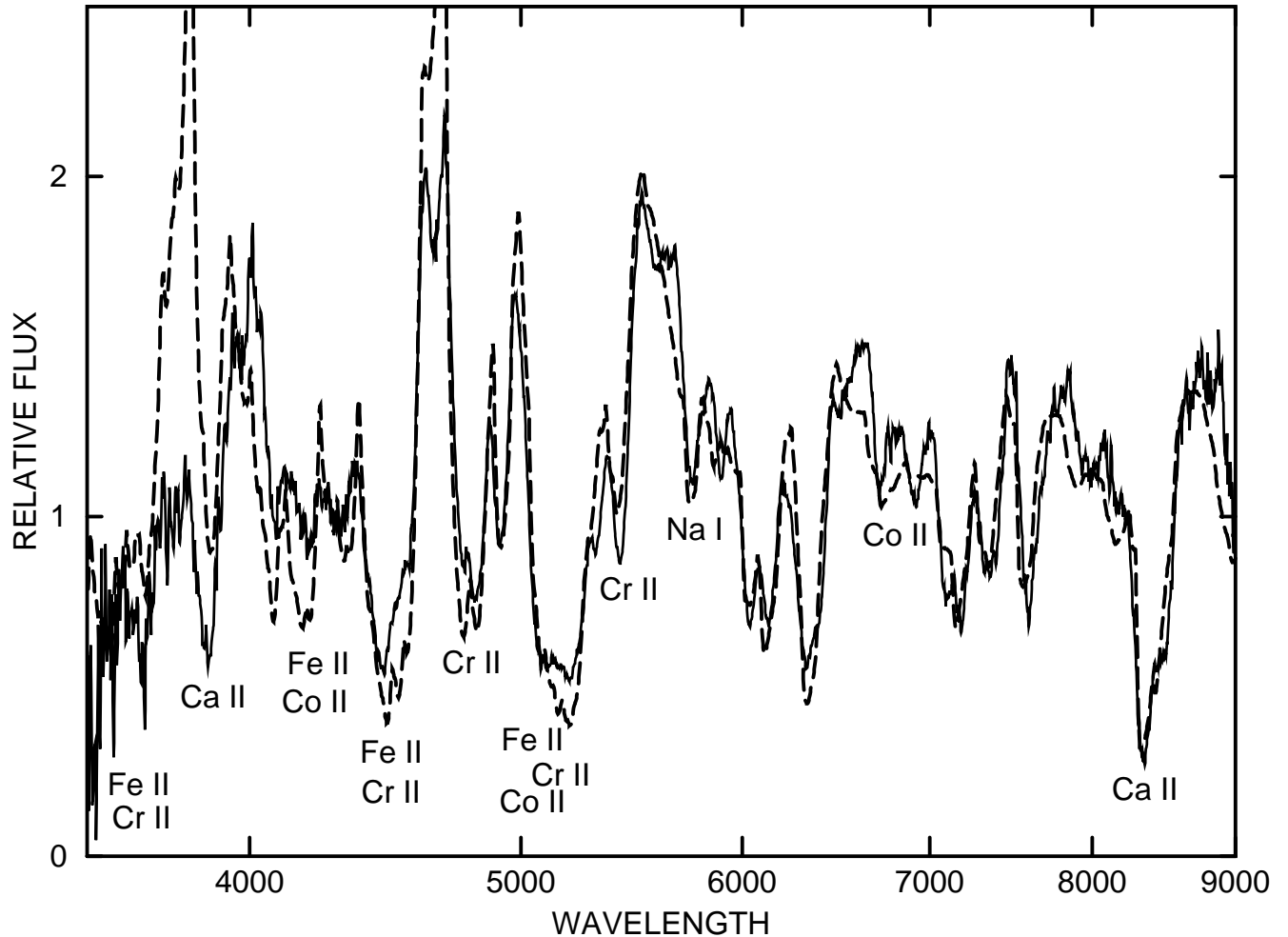


Fig. 20.— The 3 week–postmax spectrum of the SS SN 2005hk (solid line) from Stanishev et al. (2007) compared with a synthetic spectrum (dashed line). Unlabelled absorption features in the synthetic spectrum are produced by Fe II.

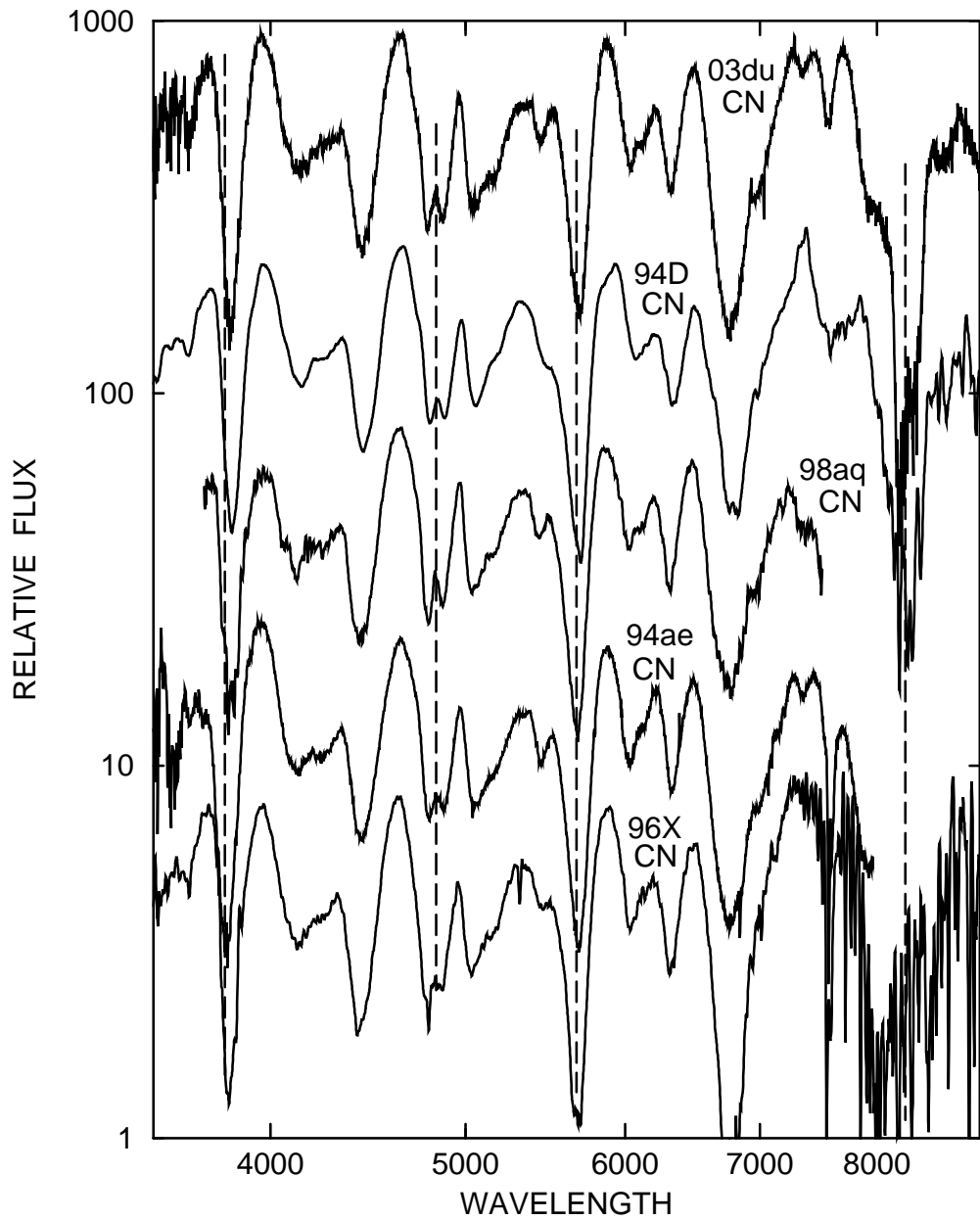


Fig. 21.— Like Fig. 2 but for the five CNs of the 3 month postmax sample.

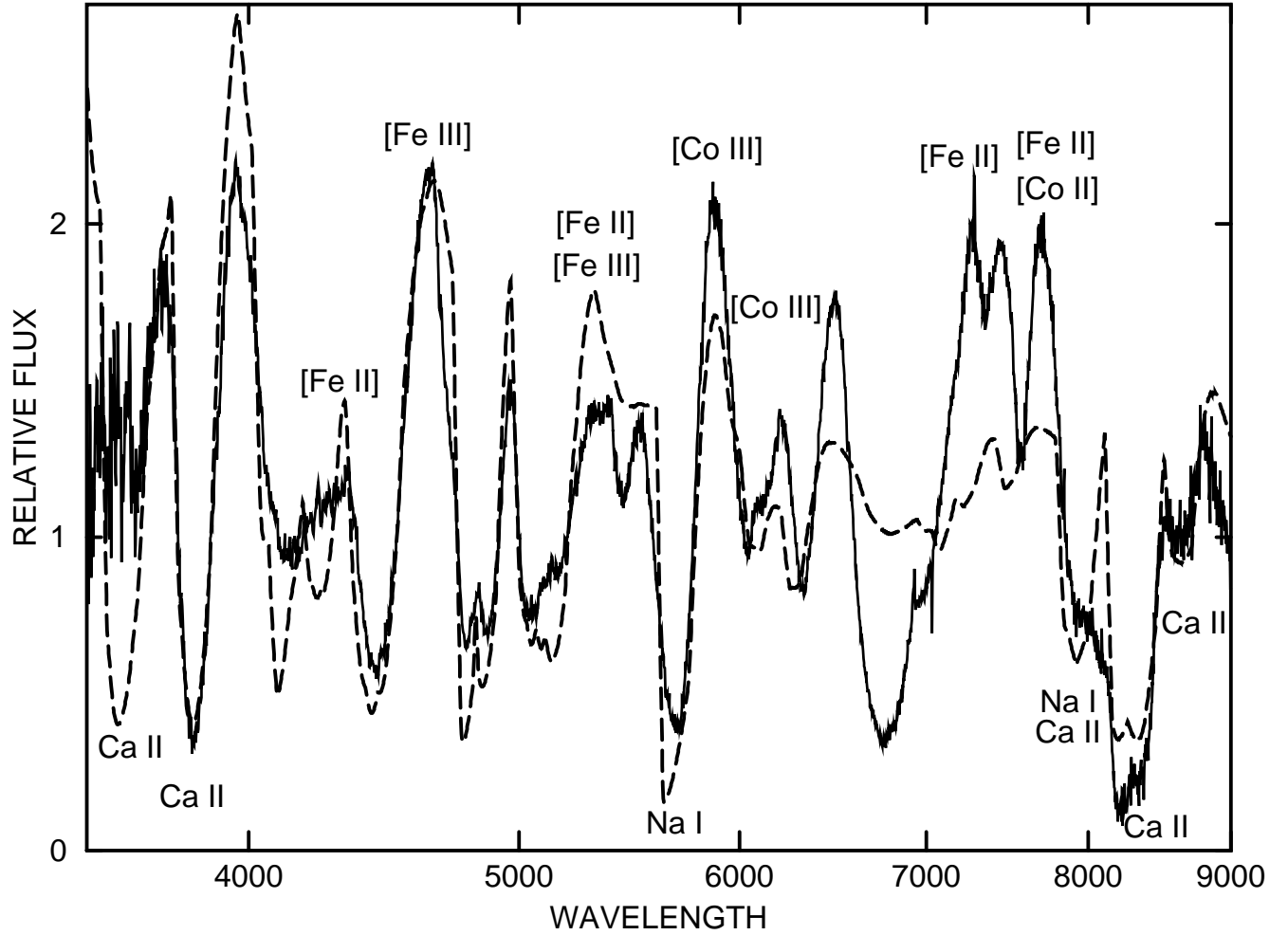


Fig. 22.— The 3 month–postmax spectrum of the CN SN 2003du (solid line) from Stanishev et al. (2007) compared with a synthetic spectrum (dashed line). The forbidden–line identifications that appear above some of the flux peaks are from Bowers et al. (1997) but these are not used in the SYNOW synthetic spectrum. Unlabelled absorption features in the synthetic spectrum are produced by Fe II.

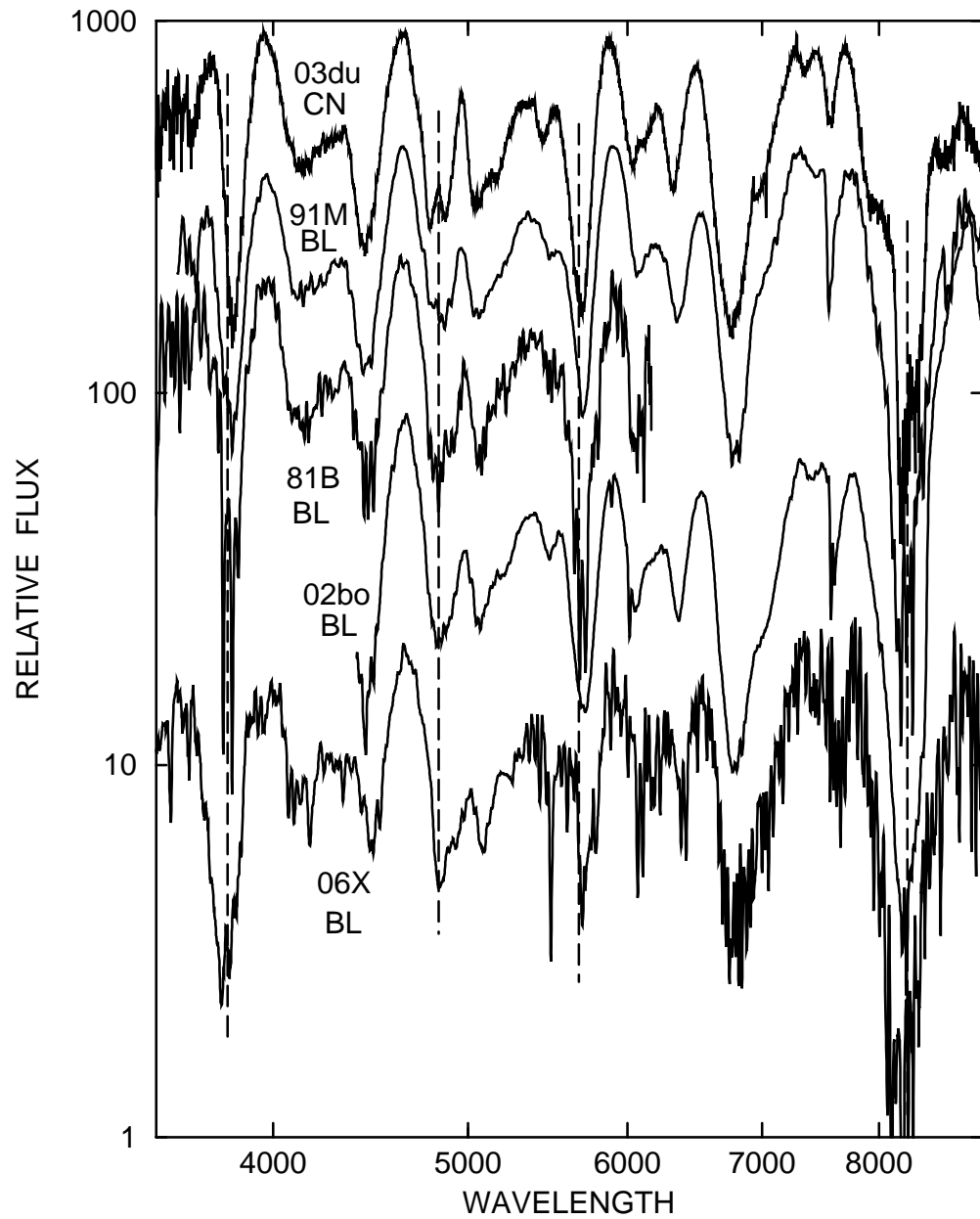


Fig. 23.— Like Fig. 2 but for one CN and the four BLs of the 3 month postmax sample.

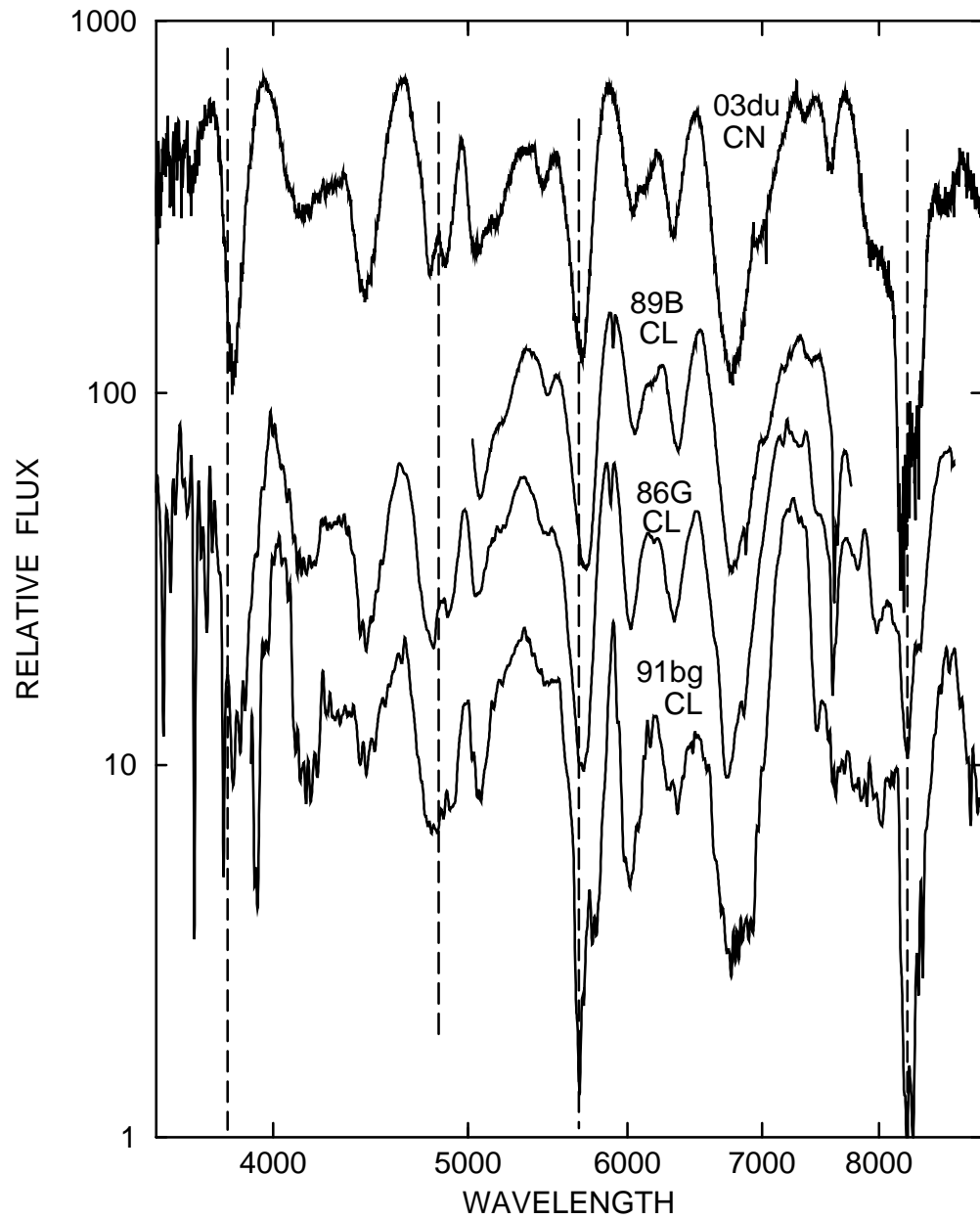


Fig. 24.— Like Fig. 2 but for one CN and the three CLs of the 3 month postmax sample.

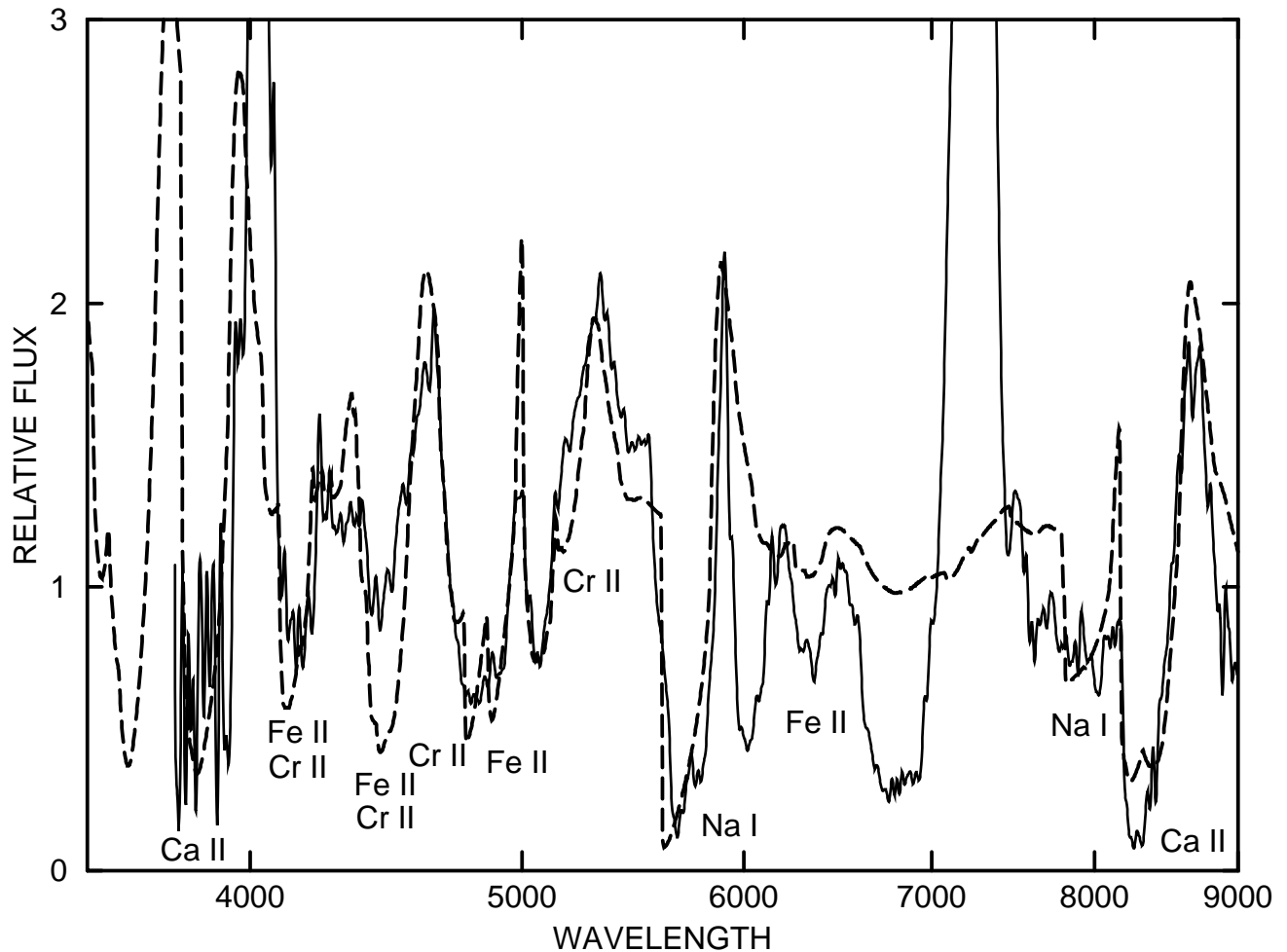


Fig. 25.— The 3 month–postmax spectrum of the CL SN 1991bg (solid line) from Filippenko et al. (1992a) compared with a synthetic spectrum (dashed line).

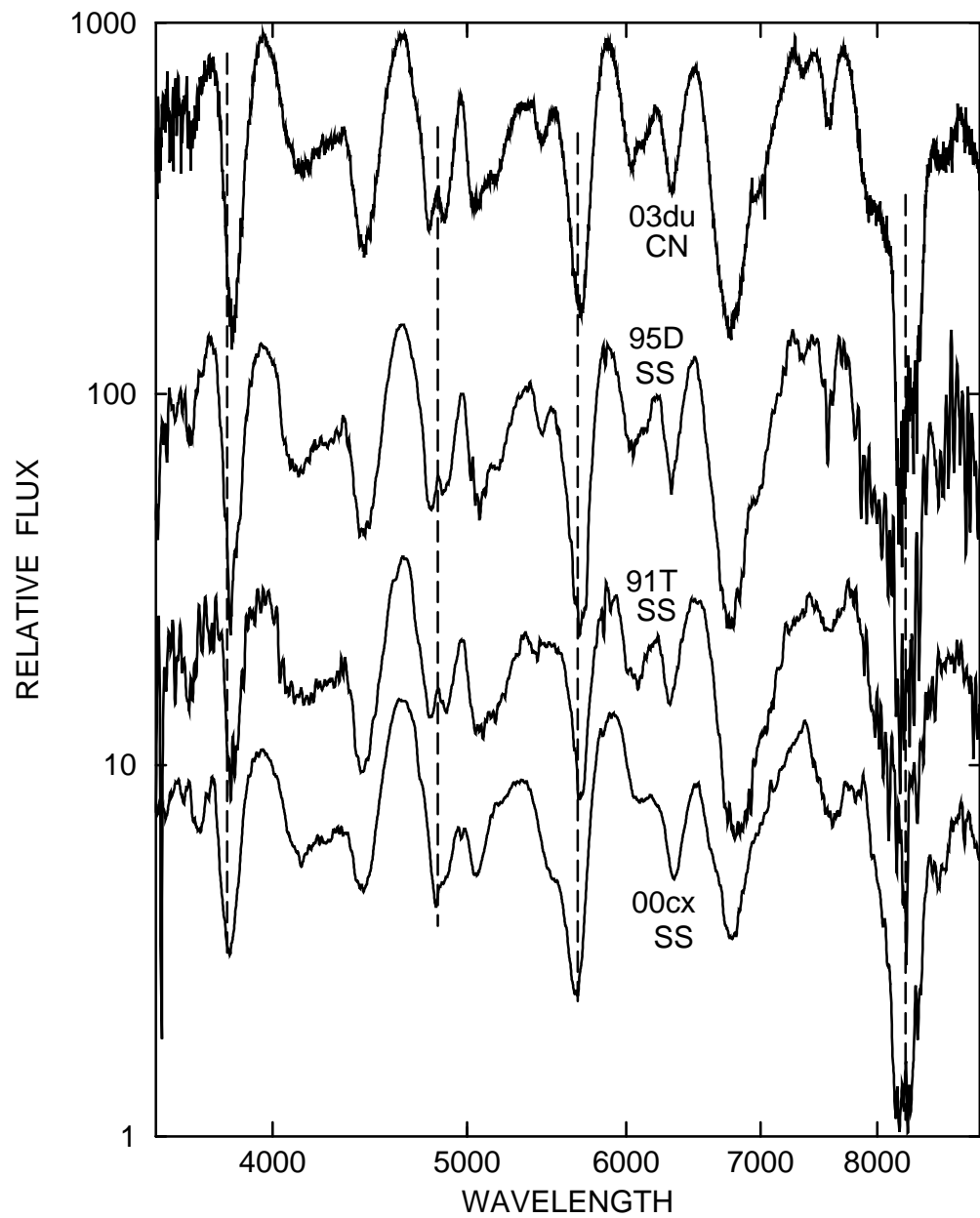


Fig. 26.— Like Fig. 2 but for one CN and the three SSs of the 3 month postmax sample.

Table 1. The SN Ia Sample

SN	Epochs (days)	Galaxy	References
1981B BL	22, 93	NGC 4526	Branch et al. 1983
1984A BL	8, 19	NGC 4419	Barbon et al. 1989
1986G CL	21, 90	NGC 5128	Cristiani et al. 1992
1989B CL	8, 19, 92	NGC 3627	Wells et al. 1994
1990N CN	7, 21	NGC 4639	7: Leibundgut et al. 1991; 21: Filippenko et al. 1992b
1991M BL	81	IC 1151	Gomez & Lopez 1998
1991T SS	83	NGC 4527	A. V. Filippenko, unpublished
1991bg CL	19, 91	NGC 4374	Filippenko et al. 1992a
1992A BL	6	NGC 1380	Kirshner et al. 1993
1994D CN	7, 19, 87	NGC 4526	7, 19: Patat et al. 1996; 87: Filippenko 1997
1994ae CN	89	NGC 3370	Bowers et al. 1997
1995D SS	96	NGC 2962	Bowers et al. 1997
1996X CN	7, 22, 87	NGC 5061	Salvo et al. 2001
1997br SS	8	ESO 576-G40	Li et al. 1999
1998aq CN	7, 21, 91	NGC 3982	Branch et al. 2003
1998bu CN	8	NGC 3368	Jha et al. 1999
1999aa SS	6, 19	NGC 4469	Garavini et al. 2004
1999ac SS	8	NGC 2848	Garavini et al. 2005
1999by CL	7	NGC 2841	Garnavich et al. 2004
1999ee SS	22	IC 5179	Hamuy et al. 2002
2000cx SS	7, 20, 89	NGC 524	Li et al. 2001
2001el CN	20	NGC 1448	Wang et al. 2003
2002bf BL	7	...	Leonard et al. 2005
2002bo BL	82	NGC 3190	Benetti et al. 2004
2002cx SS	21	...	Li et al. 2003
2002er BL	6, 20	UGC 10743	Kotak et al. 2006
2003cg CN	7, 23	NGC 3169	Elias–Rosa et al. 2006
2003du CN	7, 84	UGC 9391	Stanishev et al. 2007
2004S CN	8, 19	...	Krisciunas et al. 2007
2004eo CL	7, 21	NGC 6928	Pastorello et al. 2007

Table 1—Continued

SN	Epochs	Galaxy	References
	(days)		
2005hk SS	21	UGC 272	Stanishev et al. 2007
2006X BL	6, 98	NGC 4321	Wang et al. 2007
2006gz SS	7	IC 1277	Hicken et al. 2007

Table 2. Fitting Parameters for Selected Spectra of the 1 Week Postmax Sample

Parameter	SN 1996X CN	SN 2004S CN	SN 2002bf BL	SN 1999by CL	SN 1999ac SS	SN 2000cx SS
v_{phot} (km s $^{-1}$)	11,000	7000	11,000	6000	6000	11,000
$\tau(\text{O I})$	0.25/[17]	0.2/[16]	0.2/[15]	0.3/[14]	0.1/[16]	0.2/[17]
$\tau(\text{Na I})$	0.3/[15]	0.3/[12]	0.5/[14]	...	0.1/[14]	0.2/[13]
$\tau(\text{Mg I})$	1/[13]
$\tau(\text{Mg II})$	0.6/[15]	0.2/[13]	0.5/[14]	...
$\tau(\text{Si II})$	2/[15]	0.5/[13]	3/[21]	1.2/[12]	0.5/[14]	1/13[15]
$\tau(\text{S II})$	0.8/[13]	0.3/[11]	0.2/[15]	...	0.3/[10]	0.3/13[15]
$\tau(\text{Ca II})$	30/[17]	15/[24]	30/[23]	100/[14]	25/[20]	2/[23]
$\tau(\text{Sc II})$	2/[11]
$\tau(\text{Ti II})$	0.8/[11]	...	0.2/23[25]
$\tau(\text{Cr II})$	2/[11]	...	0.3/21[23]
$\tau(\text{Fe II})$	1/[15]	0.8/[13]	1.5/[21]	7/[11]	0.8/[15]	0.3/19[22]
$\tau(\text{Fe III})$	0.3/[15]	0.3/[13]	0.3/13[15]
$\tau(\text{Co II})$	0.6/[15]	0.6/[13]
$\tau(\text{Ni II})$	0.1/13[15]

^aNOTE.—For each ion, the optical depth τ is the optical depth at the photosphere or detachment velocity of the ion’s reference line (ordinarily the ion’s strongest line in the optical spectrum). Minimum and maximum velocities (in units of 1000 km s $^{-1}$) are preceded by a forward slash, with maximum velocities in square brackets.

Table 3. Fitting Parameters for Selected Spectra of the 3 Weeks Postmax Sample

Parameter	SN 1996X	SN 1991bg	SN 2005hk	SN 2000cx
	CN	CL	SS	SS
v_{phot} (km s $^{-1}$)	6000	6000	4000	7000
$\tau(\text{O I})$...	0.6/8[13]
$\tau(\text{Na I})$	0.4/7[17]	0.6/10[13]	0.2/6[9]	0.6/[18]
$\tau(\text{Si II})$	0.7/8[13]	1.2/7[11]	...	0.7/9[16]
$\tau(\text{Ca II})$	50/[16]	500/9[14]	50/[9]	...
$\tau(\text{Ti II})$...	3/[11]
$\tau(\text{Cr II})$	6/[13]	10/[11]	10/[8]	0.3/[18]
$\tau(\text{Fe II})$	12/[13]	10/[11]	30/[8]	0.8/[18]
$\tau(\text{Fe III})$	0.5/[15]
$\tau(\text{Co II})$	6/[13]	...	10/[8]	...

^aNOTE.—For column descriptions, see the note to Table 2.

Table 4. Fitting Parameters for Selected Spectra of the 3 Months Postmax Sample

Parameter	SN 2003du	SN 1991bg
	CN	CL
v_{phot} (km s $^{-1}$)	7000	3000
$\tau(\text{Na I})$	4/[15]	4/[15]
$\tau(\text{Ca II})$	10,000/[14]	1000/[12]
$\tau(\text{Fe II})$	8/[12]	2/[10]
$\tau(\text{Cr II})$...	0.5/[10]

^aNOTE.—For column descriptions, see the note to Table 2.